

**MULTISPECIES TOTALLY ASYMMETRIC ZERO RANGE PROCESS:
I. MULTILINE PROCESS AND COMBINATORIAL R**

ATSUO KUNIBA, SHOUYA MARUYAMA, AND MASATO OKADO

Abstract

We introduce an n -species totally asymmetric zero range process (n -TAZRP) on one-dimensional periodic lattice with L sites. It is a continuous time Markov process in which n species of particles hop to the adjacent site only in one direction under the condition that smaller species ones have the priority to do so. Also introduced is an n -line process, a companion stochastic system having the uniform steady state from which the n -TAZRP is derived as the image by a certain projection π . We construct the π by a combinatorial R of the quantum affine algebra $U_q(\widehat{sl}_L)$ and establish a matrix product formula of the steady state probability of the n -TAZRP in terms of corner transfer matrices of a $q = 0$ -oscillator valued vertex model. These results parallel the recent reformulation of the n -species totally asymmetric simple exclusion process (n -TASEP) by the authors, demonstrating that n -TAZRP and n -TASEP are the canonical sister models associated with the symmetric and the antisymmetric tensor representations of $U_q(\widehat{sl}_L)$ at $q = 0$, respectively.

1. INTRODUCTION

Zero range processes are stochastic dynamical systems modeling a variety of nonequilibrium phenomena in biology, chemistry, economics, networks, physics, sociology and so forth. In this article and the next [19] we introduce and study a new zero range process on one-dimensional (1D) periodic lattice of length L . There are n species of particles living on the sites with no constraint on their occupation numbers. Particles within a site hop to the left adjacent site or remain unmoved under the condition that smaller species ones have the priority to hop. We call it *n -species totally asymmetric zero range process* (n -TAZRP), where TA refers to the unidirectional move and ZR signifies that the interaction of particles via the priority constraint works only among those occupying the same departure site. A cheerful realization of such a system is children's play along a circle divided into L segments. The species of particles are interpreted as ages of the children. They are allowed to move forward to the next segment only when accompanying all the strictly younger fellows than themselves to look after. As one may imagine from such an example there is a general tendency of *condensation*, whose symptom is indeed observed in our TAZRP. See Example 2.1.

There are several kinds of one-dimensional zero range processes studied in the literature. They are mostly one or two-species models. See for example [7, 22, 3] and references therein. The n -TAZRP in this article and [19] is the first multispecies example which allows an explicit matrix product formula for the steady state probability for general $n \geq 1$. It possesses a number of distinctive features summarized below.

(i) Our n -TAZRP is the image of a certain projection π from another stochastic system, the *n -line process* (n -LP), which we also introduce in this paper. It has the steady state with uniform probability distribution. Denoting their Markov matrices by H_{TAZRP} and H_{LP} respectively, we have the intertwining relation

$$\pi H_{\text{LP}} = H_{\text{TAZRP}} \pi.$$

The map π is a source of many intriguing features in our construction. It is realized as a composition of a *combinatorial R* [21] of the quantum affine algebra $U_q(\widehat{\mathfrak{sl}}_L)$ [5, 12]. The combinatorial R is a bijection between finite sets called *crystals* and arises as a quantum R matrix at $q = 0$ [14, 15, 10]. Systematic use of the Yang-Baxter equation [1] satisfied by the combinatorial R is a key maneuver in our working. In particular the projection π admits a queueing type description (Section 4.4) analogous to the Ferrari-Martin algorithm [8] for the n -species totally asymmetric simple exclusion process (n -TASEP).

(ii) Our main result, Theorem 5.8, is a matrix product formula of the steady state probability of the configuration $(\sigma_1, \dots, \sigma_L)$ of the n -TAZRP:

$$\mathbb{P}(\sigma_1, \dots, \sigma_L) = \text{Tr}(X_{\sigma_1} \cdots X_{\sigma_L}).$$

The operator X_σ assigned with a local state σ is a configuration sum that can be viewed as a *corner transfer matrix* [1] of a $q = 0$ -oscillator valued vertex model. It acts on the $n(n-1)/2$ -fold tensor product of the $q = 0$ -oscillator Fock space. See (5.10). The X_σ can also be regarded as a layer-to-layer transfer matrix of a 3D lattice model, and $\mathbb{P}(\sigma_1, \dots, \sigma_L)$ is thereby interpreted as a *partition function* of the 3D model with prism shape under a prescribed boundary condition.

(iii) By extending the setting to generic q , the corner transfer matrix X_σ is naturally embedded into a layer-to-layer transfer matrix of a more general 3D lattice model. Then the most local hence fundamental relation responsible for the steady state condition turns out to be the *tetrahedron equation* [25], which is a 3D generalization of the Yang-Baxter equation. The result reveals the 3D integrability in the matrix product construction.

(iv) Our n -TAZRP is a model in which the “physical space” is of size L and the “internal space” is of size n . In contrast, the internal symmetry of the combinatorial R is $U_{q=0}(\widehat{\mathfrak{sl}}_L)$ and the system size of the corner transfer matrix is n . See Theorem 5.2. In particular the cyclic symmetry \mathbb{Z}_L of the original lattice has been incorporated into the Dynkin diagram of the internal symmetry algebra $U_q(\widehat{\mathfrak{sl}}_L)$. In this sense our approach captures the *cross channel* of the original problem where the two kinds of spaces and symmetries are interchanged. It is a manifestation of the *rank-size duality* commonly recognized for a class of 3D systems associated with the tetrahedron equation [2, 20]. We stress that such a hidden 3D structure can be elucidated only by a systematic investigation on the multispecies case $n \geq 1$. An alternative approach via the direct channel based on some rank n internal symmetry algebra is yet to be undertaken.

(v) The whole story about the n -TAZRP in this paper and [19] is closely parallel with the recent result on the n -TASEP by the authors [17, 18]. In fact the n -TAZRP and the n -TASEP turn out to be the canonical sister models associated with the symmetric and the antisymmetric tensor representations of $U_q(\widehat{\mathfrak{sl}}_L)$ at $q = 0$, respectively. The combinatorial R 's for both of them had been obtained in [21]. In terms of the 3D picture, the two models are associated with 3D R -operator and the 3D L -operator, respectively. They are distinguished solutions to the tetrahedron equation which have a rich background going back to the representation theory of the quantized algebra of functions [13]. See [2, 20, 16] and references therein.

In this paper we will demonstrate the features (i) and (ii) of combinatorial nature mainly, and leave the issue (iii) related to the tetrahedron equation to the subsequent paper [19]. Although the main idea comes from the crystal base theory, a theory of quantum groups at $q = 0$ [14, 10], the article has been designed to be readable without knowledge of it.

In Section 2 the n -TAZRP is defined and examples of the steady states are presented. In Section 3 the n -line process is introduced on the set $B(\mathbf{m})$ which is the crystal of the n -fold tensor product of the symmetric tensor representation of $U_q(\widehat{\mathfrak{sl}}_L)$. It is shown that the steady state of the n -line process has the uniform probability distribution (Theorem 3.6). In Section 4 the projection π from the n -line process to the n -TAZRP is constructed from a composition of the combinatorial R . It is also described in terms of a multiple queueing type algorithm in Section 4.4, which contrasts with the analogous procedure for TASEP [8, 17]. The steady state of the n -TAZRP is the image of the uniform state in the n -line process. In Section 5 a matrix product formula for the steady

state probability is derived for the n -TAZRP, which is expressed by corner transfer matrices of $q = 0$ -oscillator valued vertex model.

Throughout the paper we use the characteristic function θ defined by $\theta(\text{true}) = 1, \theta(\text{false}) = 0$.

2. n -TAZRP

2.1. Definition of n -TAZRP. Consider a periodic one-dimensional chain \mathbb{Z}_L with L sites. Each site $i \in \mathbb{Z}_L$ is assigned with a local state $\sigma_i = (\sigma_i^1, \dots, \sigma_i^n) \in (\mathbb{Z}_{\geq 0})^n$ which is interpreted as an assembly of n species of particles as

$$\left| \overbrace{1 \dots 1}^{\sigma_i^1} \overbrace{2 \dots 2}^{\sigma_i^2} \dots \overbrace{n \dots n}^{\sigma_i^n} \right| \quad (2.1)$$

The ordering of particles within a site does not matter. A local state α is specified uniquely either by *multiplicity representation* $\alpha = (\alpha^1, \dots, \alpha^n) \in (\mathbb{Z}_{\geq 0})^n$ as above or *multiset representation* $\alpha = (\alpha_1, \dots, \alpha_r) \in [1, n]^r$ with $1 \leq \alpha_1 \leq \dots \leq \alpha_r \leq n$. They are related by $\alpha^a = \#\{j \in [1, r] \mid \alpha_j = a\}$ and $r = |\alpha| := \alpha^1 + \dots + \alpha^n$.

Let (α, β) and (γ, δ) be pairs of local states. Let $(\beta_1, \dots, \beta_r)$ be the multiset representation of β , hence $1 \leq \beta_1 \leq \dots \leq \beta_r \leq n$. For the two pairs we define $>$ by

$$(\alpha, \beta) > (\gamma, \delta) \stackrel{\text{def}}{\iff} \gamma = \alpha \cup \{\beta_1, \dots, \beta_k\}, \delta = (\beta_{k+1}, \dots, \beta_r) \text{ for some } k \in [1, r], \quad (2.2)$$

where $\alpha \cup \{\beta_1, \dots, \beta_k\}$ is a union as a multiset. For instance in multiset representation we have¹

$$\begin{aligned} (1356, 114) &> (11356, 14), (111356, 4), (1113456, \emptyset), \\ (235, 12446) &> (1235, 2446), (12235, 446), (122345, 46), (1223445, 6), (12234456, \emptyset), \\ (\emptyset, 225) &> (2, 25), (22, 5), (225, \emptyset), \\ (344, \emptyset) &> \text{none}. \end{aligned} \quad (2.3)$$

We let $(\alpha, \beta) \geq (\gamma, \delta)$ mean $(\alpha, \beta) > (\gamma, \delta)$ or $(\alpha, \beta) = (\gamma, \delta)$.

By n -TAZRP we mean a stochastic process on \mathbb{Z}_L in which neighboring pairs of local states $(\sigma_i, \sigma_{i+1}) = (\alpha, \beta)$ change into (γ, δ) such that $(\alpha, \beta) > (\gamma, \delta)$ with a uniform transition rate. For example the first line in (2.3) implies that the following local transitions take place with an equal rate:

$$\begin{array}{c} \begin{array}{c} 1 \\ \downarrow \\ \boxed{1356 \mid 114} \end{array} \rightarrow \boxed{11356 \mid 14} \\ \begin{array}{c} 11 \\ \downarrow \\ \boxed{1356 \mid 114} \end{array} \rightarrow \boxed{111356 \mid 4} \\ \begin{array}{c} 114 \\ \downarrow \\ \boxed{1356 \mid 114} \end{array} \rightarrow \boxed{1113456 \mid} \end{array}$$

In general we let $\tau_i^k : (\sigma_1, \dots, \sigma_L) \mapsto (\sigma'_1, \dots, \sigma'_L)$ denote the transition (2.2) in which smaller species k particles move from the $(i+1)$ -th site to the i -th site with no change elsewhere:

$$\tau_i^k : \begin{array}{c} \overbrace{\alpha_1 \dots \alpha_s \mid \beta_1 \dots \beta_r}^{\beta_1 \dots \beta_k} \\ \downarrow \\ \boxed{\alpha_1 \dots \alpha_s \mid \beta_1 \dots \beta_r} \end{array} \rightarrow \boxed{\alpha_1 \dots \alpha_s \beta_1 \dots \beta_k \mid \beta_{k+1} \dots \beta_r} \quad (2.4)$$

$\sigma_i \qquad \qquad \qquad \sigma_{i+1} \qquad \qquad \qquad \sigma'_i \qquad \qquad \qquad \sigma'_{i+1}$

¹ Here and in what follows, a multiset (set accounting for multiplicity of elements), say $\{1, 1, 3, 5, 6\}$, is abbreviated to 11356, which does not cause a confusion since all the examples in this paper shall be concerned with the case $n \leq 9$.

where $1 \leq \beta_1 \leq \dots \leq \beta_r \leq n$, $k \in [1, r]$, $i \in \mathbb{Z}_L$, and $\sigma'_j = \sigma_j$ for $j \neq i, i+1$. For a later convenience we extend τ_i^k to all $k \in \mathbb{Z}_{\geq 1}$ by setting $\tau_i^k = 1$ for $k > r$ which means to move no particle.

This dynamics is *totally asymmetric* in that particles can hop only to the left adjacent site. Their interaction is of *zero range* in that the hopping priority for smaller species particles is respected only among those occupying the same site. There is no constraint on the status of the destination site nor number of particles that hop at a transition. A pair (α, β) of adjacent local states has $|\beta|$ possibilities to change into.

The n -TAZRP dynamics obviously preserves the number of particles of each species. Thus we introduce *sectors* labeled with *multiplicity* $\mathbf{m} = (m_1, \dots, m_n) \in (\mathbb{Z}_{\geq 0})^n$ of the species of particles:

$$S(\mathbf{m}) = \{\boldsymbol{\sigma} = (\sigma_1, \dots, \sigma_L) \mid \sigma_i = (\sigma_i^1, \dots, \sigma_i^n) \in (\mathbb{Z}_{\geq 0})^n, \sum_{i=1}^L \sigma_i^a = m_a, \forall a \in [1, n]\}. \quad (2.5)$$

A configuration will also be written as $\boldsymbol{\sigma} = (\sigma_i^a)$. A sector $S(\mathbf{m})$ such that $m_a \geq 1$ for all $a \in [1, n]$ is called *basic*. Non-basic sectors are equivalent to a basic sector for n' -TAZRP with some $n' < n$ by a suitable relabeling of species. Thus we shall exclusively deal with basic sectors in this paper.

A local state σ_i in (2.5) can take $N = \prod_{a=1}^n (m_a + 1)$ possibilities in view of (2.1). Let $\{|\boldsymbol{\sigma}\rangle = |\sigma_1, \dots, \sigma_L\rangle\}$ be a basis of $(\mathbb{C}^N)^{\otimes L}$. Denoting by $\mathbb{P}(\sigma_1, \dots, \sigma_L; t)$ the probability of finding the system in the configuration $\boldsymbol{\sigma} = (\sigma_1, \dots, \sigma_L)$ at time t , we set

$$|P(t)\rangle = \sum_{\boldsymbol{\sigma} \in S(\mathbf{m})} \mathbb{P}(\sigma_1, \dots, \sigma_L; t) |\sigma_1, \dots, \sigma_L\rangle.$$

This actually belongs to a subspace of $(\mathbb{C}^N)^{\otimes L}$ of dimension $\#S(\mathbf{m}) = \prod_{a=1}^n \binom{L+m_a-1}{m_a}$ which is in general much smaller than N^L reflecting the constraint in (2.5).

Our n -TAZRP is a stochastic system governed by the continuous-time master equation

$$\frac{d}{dt}|P(t)\rangle = H_{\text{TAZRP}}|P(t)\rangle,$$

where the Markov matrix has the form

$$H_{\text{TAZRP}} = \sum_{i \in \mathbb{Z}_L} h_{i, i+1}, \quad h|\alpha, \beta\rangle = \sum_{\gamma, \delta} h_{\alpha, \beta}^{\gamma, \delta} |\gamma, \delta\rangle. \quad (2.6)$$

Here $h_{i, i+1}$ is the local Markov matrix that acts as h on the i -th and the $(i+1)$ -th components nontrivially and as the identity elsewhere. If the transition rate of the adjacent pair of local states $(\alpha, \beta) \rightarrow (\gamma, \delta)$ is denoted by $w(\alpha\beta \rightarrow \gamma\delta)$, the matrix element of the Markov matrix is given by $h_{\alpha, \beta}^{\gamma, \delta} = w(\alpha\beta \rightarrow \gamma\delta) - \theta((\alpha, \beta) = (\gamma, \delta)) \sum_{\gamma', \delta'} w(\alpha\beta \rightarrow \gamma'\delta')$. Our n -TAZRP corresponds to the choice $w(\alpha\beta \rightarrow \gamma\delta) = \theta((\alpha, \beta) > (\gamma, \delta))$, therefore the general formula, which is independent of $w(\alpha\beta \rightarrow \alpha\beta)$, gives

$$h_{\alpha, \beta}^{\gamma, \delta} = \begin{cases} 1 & \text{if } (\alpha, \beta) > (\gamma, \delta), \\ -|\beta| & \text{if } (\alpha, \beta) = (\gamma, \delta), \\ 0 & \text{otherwise.} \end{cases}$$

The Markov matrix (2.6) is expressed as

$$H_{\text{TAZRP}} = \sum_{i \in \mathbb{Z}_L} \sum_{k \geq 1} (\tau_i^k - 1), \quad (2.7)$$

which is actually a finite sum due to the convention explained after (2.4).

2.2. Steady state. As time goes on, the distribution of the particles converges to the state that we consider from now on. Given a system size L and a sector $S(\mathbf{m})$ there is a unique vector

$$|\bar{P}_L(\mathbf{m})\rangle = \sum_{\boldsymbol{\sigma} \in S(\mathbf{m})} \mathbb{P}(\boldsymbol{\sigma}) |\boldsymbol{\sigma}\rangle \quad (2.8)$$

up to a normalization, called the *steady state*, which satisfies $H_{\text{TAZRP}}|\bar{P}_L(\mathbf{m})\rangle = 0$ hence is time-independent. In what follows we will always take $\mathbb{P}(\boldsymbol{\sigma})$ so that

$$\sum_{\boldsymbol{\sigma} \in S(\mathbf{m})} \mathbb{P}(\boldsymbol{\sigma}) = \#B(\mathbf{m})$$

holds, where $\#B(\mathbf{m})$ is given by (3.3) and (3.1). The unnormalized $\mathbb{P}(\boldsymbol{\sigma})$ will be called the steady state probability by abusing the terminology. The properly normalized one is equal to $\mathbb{P}_{\text{normalized}}(\boldsymbol{\sigma}) = \mathbb{P}(\boldsymbol{\sigma})/(\#B(\mathbf{m}))$. This convention is convenient for our working below in that $\mathbb{P}(\boldsymbol{\sigma}) \in \mathbb{Z}_{\geq 1}$ holds as we will see in Theorem 4.8 and (5.1).

The steady state for 1-TAZRP is trivial under the present periodic boundary condition in that all the configurations are realized with an equal probability.

Example 2.1. We present the steady state in small sectors of 2-TAZRP and 3-TAZRP in the form

$$|\bar{P}_L(\mathbf{m})\rangle = |\xi_L(\mathbf{m})\rangle + C|\xi_L(\mathbf{m})\rangle + \cdots + C^{L-1}|\xi_L(\mathbf{m})\rangle$$

respecting the symmetry $H_{\text{TAZRP}}C = CH_{\text{TAZRP}}$ under the \mathbb{Z}_L cyclic shift $C : |\sigma_1, \sigma_2, \dots, \sigma_L\rangle \mapsto |\sigma_L, \sigma_1, \dots, \sigma_{L-1}\rangle$. The choice of the vector $|\xi_L(\mathbf{m})\rangle$ is not unique. We employ multiset representation like $|\emptyset, 3, 122\rangle$, which would have looked as $|000, 001, 120\rangle$ in the multiplicity representation for 3-TAZRP.

For the 2-TAZRP one has

$$\begin{aligned} |\xi_2(1, 1)\rangle &= 2|\emptyset, 12\rangle + |1, 2\rangle, \\ |\xi_3(1, 1)\rangle &= 3|\emptyset, \emptyset, 12\rangle + 2|\emptyset, 1, 2\rangle + |\emptyset, 2, 1\rangle, \\ |\xi_4(1, 1)\rangle &= 4|\emptyset, \emptyset, \emptyset, 12\rangle + 3|\emptyset, \emptyset, 1, 2\rangle + 2|\emptyset, 1, \emptyset, 2\rangle + |\emptyset, \emptyset, 2, 1\rangle, \\ |\xi_2(2, 1)\rangle &= 2|\emptyset, 112\rangle + |1, 12\rangle + |2, 11\rangle, \\ |\xi_3(2, 1)\rangle &= 3|\emptyset, \emptyset, 112\rangle + 2|\emptyset, 1, 12\rangle + |\emptyset, 2, 11\rangle + 2|\emptyset, 11, 2\rangle + |\emptyset, 12, 1\rangle + |1, 1, 2\rangle, \\ |\xi_4(2, 1)\rangle &= 2|\emptyset, 1, 1, 2\rangle + |\emptyset, 1, 2, 1\rangle + 2|\emptyset, 1, \emptyset, 12\rangle + |\emptyset, 2, 1, 1\rangle + 2|\emptyset, 2, \emptyset, 11\rangle + 3|\emptyset, \emptyset, 1, 12\rangle \\ &\quad + |\emptyset, \emptyset, 2, 11\rangle + 3|\emptyset, \emptyset, 11, 2\rangle + |\emptyset, \emptyset, 12, 1\rangle + 4|\emptyset, \emptyset, \emptyset, 112\rangle, \\ |\xi_2(1, 2)\rangle &= 3|\emptyset, 122\rangle + |1, 22\rangle + 2|2, 12\rangle, \\ |\xi_3(1, 2)\rangle &= 6|\emptyset, \emptyset, 122\rangle + 3|\emptyset, 1, 22\rangle + 3|\emptyset, 2, 12\rangle + 5|\emptyset, 12, 2\rangle + |\emptyset, 22, 1\rangle + 2|1, 2, 2\rangle, \\ |\xi_4(1, 2)\rangle &= 5|\emptyset, 1, 2, 2\rangle + 3|\emptyset, 1, \emptyset, 22\rangle + 3|\emptyset, 2, 1, 2\rangle + 2|\emptyset, 2, 2, 1\rangle + 7|\emptyset, 2, \emptyset, 12\rangle + 6|\emptyset, \emptyset, 1, 22\rangle \\ &\quad + 4|\emptyset, \emptyset, 2, 12\rangle + 9|\emptyset, \emptyset, 12, 2\rangle + |\emptyset, \emptyset, 22, 1\rangle + 10|\emptyset, \emptyset, \emptyset, 122\rangle, \\ |\xi_2(3, 1)\rangle &= 2|\emptyset, 1112\rangle + |1, 112\rangle + |2, 111\rangle + |11, 12\rangle, \\ |\xi_3(3, 1)\rangle &= 3|\emptyset, \emptyset, 1112\rangle + 2|\emptyset, 1, 112\rangle + |\emptyset, 2, 111\rangle + 2|\emptyset, 11, 12\rangle + |\emptyset, 12, 11\rangle \\ &\quad + 2|\emptyset, 111, 2\rangle + |\emptyset, 112, 1\rangle + |1, 1, 12\rangle + |1, 2, 11\rangle + |1, 11, 2\rangle, \\ |\xi_2(2, 2)\rangle &= 3|\emptyset, 1122\rangle + |1, 122\rangle + 2|2, 112\rangle + |11, 22\rangle + \frac{1}{2}|12, 12\rangle, \\ |\xi_3(2, 2)\rangle &= |1, 1, 22\rangle + |1, 2, 12\rangle + 2|1, 12, 2\rangle + 2|2, 2, 11\rangle + 3|\emptyset, 1, 122\rangle + 3|\emptyset, 2, 112\rangle \\ &\quad + 3|\emptyset, 11, 22\rangle + 2|\emptyset, 12, 12\rangle + |\emptyset, 22, 11\rangle + 5|\emptyset, 112, 2\rangle + |\emptyset, 122, 1\rangle + 6|\emptyset, \emptyset, 1122\rangle, \\ |\xi_2(1, 3)\rangle &= |1, 222\rangle + 3|2, 122\rangle + 2|12, 22\rangle + 4|\emptyset, 1222\rangle, \\ |\xi_3(1, 3)\rangle &= 2|1, 2, 22\rangle + 3|1, 22, 2\rangle + 5|2, 2, 12\rangle + 4|\emptyset, 1, 222\rangle + 6|\emptyset, 2, 122\rangle + 7|\emptyset, 12, 22\rangle \\ &\quad + 3|\emptyset, 22, 12\rangle + 9|\emptyset, 122, 2\rangle + |\emptyset, 222, 1\rangle + 10|\emptyset, \emptyset, 1222\rangle. \end{aligned}$$

Although $|\xi_2(2, 2)\rangle$ contains $\frac{1}{2}|12, 12\rangle$, the coefficients in $|\bar{P}_2(2, 2)\rangle$ are integers as this configuration is an order 2 fixed point of C .

For the 3-TAZRP one has

$$\begin{aligned}
|\xi_2(1, 1, 1)\rangle &= 2|1, 23\rangle + |2, 13\rangle + 3|3, 12\rangle + 6|\emptyset, 123\rangle, \\
|\xi_3(1, 1, 1)\rangle &= 5|1, 2, 3\rangle + |1, 3, 2\rangle + 9|\emptyset, 1, 23\rangle + 3|\emptyset, 2, 13\rangle + 6|\emptyset, 3, 12\rangle + 12|\emptyset, 12, 3\rangle \\
&\quad + 3|\emptyset, 13, 2\rangle + 3|\emptyset, 23, 1\rangle + 18|\emptyset, \emptyset, 123\rangle, \\
|\xi_4(1, 1, 1)\rangle &= 17|\emptyset, 1, 2, 3\rangle + 3|\emptyset, 1, 3, 2\rangle + 12|\emptyset, 1, \emptyset, 23\rangle + 3|\emptyset, 2, 1, 3\rangle + 7|\emptyset, 2, 3, 1\rangle + 8|\emptyset, 2, \emptyset, 13\rangle \\
&\quad + 9|\emptyset, 3, 1, 2\rangle + |\emptyset, 3, 2, 1\rangle + 20|\emptyset, 3, \emptyset, 12\rangle + 24|\emptyset, \emptyset, 1, 23\rangle + 6|\emptyset, \emptyset, 2, 13\rangle + 10|\emptyset, \emptyset, 3, 12\rangle \\
&\quad + 30|\emptyset, \emptyset, 12, 3\rangle + 6|\emptyset, \emptyset, 13, 2\rangle + 4|\emptyset, \emptyset, 23, 1\rangle + 40|\emptyset, \emptyset, \emptyset, 123\rangle, \\
|\xi_2(2, 1, 1)\rangle &= 2|1, 123\rangle + |2, 113\rangle + 3|3, 112\rangle + 2|11, 23\rangle + |12, 13\rangle + 6|\emptyset, 1123\rangle, \\
|\xi_3(2, 1, 1)\rangle &= 3|1, 1, 23\rangle + 2|1, 2, 13\rangle + |1, 3, 12\rangle + 5|1, 12, 3\rangle + |1, 13, 2\rangle + 5|2, 3, 11\rangle + |2, 11, 3\rangle \\
&\quad + 9|\emptyset, 1, 123\rangle + 3|\emptyset, 2, 113\rangle + 6|\emptyset, 3, 112\rangle + 9|\emptyset, 11, 23\rangle + 3|\emptyset, 12, 13\rangle + 3|\emptyset, 13, 12\rangle \\
&\quad + 3|\emptyset, 23, 11\rangle + 12|\emptyset, 112, 3\rangle + 3|\emptyset, 113, 2\rangle + 3|\emptyset, 123, 1\rangle + 18|\emptyset, \emptyset, 1123\rangle, \\
|\xi_2(1, 2, 1)\rangle &= 2|1, 223\rangle + 2|2, 123\rangle + 4|3, 122\rangle + 3|12, 23\rangle + |13, 22\rangle + 8|\emptyset, 1223\rangle, \\
|\xi_3(1, 2, 1)\rangle &= 5|1, 2, 23\rangle + |1, 3, 22\rangle + 7|1, 22, 3\rangle + 2|1, 23, 2\rangle + 3|2, 2, 13\rangle + 9|2, 3, 12\rangle + 3|2, 12, 3\rangle \\
&\quad + 12|\emptyset, 1, 223\rangle + 8|\emptyset, 2, 123\rangle + 10|\emptyset, 3, 122\rangle + 17|\emptyset, 12, 23\rangle + 4|\emptyset, 13, 22\rangle + 3|\emptyset, 22, 13\rangle \\
&\quad + 6|\emptyset, 23, 12\rangle + 20|\emptyset, 122, 3\rangle + 7|\emptyset, 123, 2\rangle + 3|\emptyset, 223, 1\rangle + 30|\emptyset, \emptyset, 1223\rangle, \\
|\xi_2(1, 1, 2)\rangle &= 3|1, 233\rangle + |2, 133\rangle + 8|3, 123\rangle + 4|12, 33\rangle + 2|13, 23\rangle + 12|\emptyset, 1233\rangle, \\
|\xi_3(1, 1, 2)\rangle &= 9|1, 2, 33\rangle + 3|1, 3, 23\rangle + 17|1, 23, 3\rangle + |1, 33, 2\rangle + 7|2, 3, 13\rangle + 3|2, 13, 3\rangle + 20|3, 3, 12\rangle \\
&\quad + 24|\emptyset, 1, 233\rangle + 6|\emptyset, 2, 133\rangle + 30|\emptyset, 3, 123\rangle + 30|\emptyset, 12, 33\rangle + 12|\emptyset, 13, 23\rangle + 8|\emptyset, 23, 13\rangle \\
&\quad + 10|\emptyset, 33, 12\rangle + 50|\emptyset, 123, 3\rangle + 4|\emptyset, 133, 2\rangle + 6|\emptyset, 233, 1\rangle + 60|\emptyset, \emptyset, 1233\rangle.
\end{aligned}$$

As these coefficients indicate, steady states are highly nontrivial for n -TAZRP with $n \geq 2$. The main issue in the subsequent sections is to characterize them in terms of the n -line process and the combinatorial R . Note that the maximally localized configuration like $60|\emptyset, \emptyset, 1233\rangle$ just above and their cyclic permutations have the largest probability. It is a symptom of *condensation* generally expected in the zero-range processes [7]. See (4.11) for the result on the general case.

3. n -LINE PROCESS

3.1. n -line states. Fix the multiplicity array \mathbf{m} and ℓ_1, \dots, ℓ_n as

$$\mathbf{m} = (m_1, \dots, m_n) \in (\mathbb{Z}_{\geq 1})^n, \quad \ell_a = m_a + m_{a+1} + \dots + m_n \quad (1 \leq a \leq n) \quad (3.1)$$

so that $\ell_1 > \ell_2 > \dots > \ell_n \geq 1$. Associated with these data we introduce the finite sets

$$\begin{aligned}
B(\mathbf{m}) &= B_{\ell_1} \otimes \dots \otimes B_{\ell_n}, \\
B_\ell &= \{(x_1, \dots, x_L) \in (\mathbb{Z}_{\geq 0})^L \mid x_1 + \dots + x_L = \ell\} \quad (\ell \in \mathbb{Z}_{\geq 1}),
\end{aligned} \quad (3.2)$$

where \otimes may just be regarded as the product of sets. By the definition we have

$$\#B(\mathbf{m}) = \prod_{a=1}^n \binom{L-1+\ell_a}{\ell_a}. \quad (3.3)$$

The sets B_ℓ and $B(\mathbf{m})$ will be called *crystals* bearing in mind, though not utilized significantly in this paper, that they can be endowed with the structure of the $U_q(\widehat{sl}_L)$ -*crystals* of the ℓ -fold symmetric tensor representation and their tensor product, respectively [14, 10].

Our n -line process is a stochastic dynamical system on $B(\mathbf{m})$. Its elements will be called *n -line states* and denoted by

$$\mathbf{x} = \mathbf{x}^1 \otimes \dots \otimes \mathbf{x}^n \in B(\mathbf{m}), \quad \mathbf{x}^a = (x_1^a, \dots, x_L^a) \in B_{\ell_a}. \quad (3.4)$$

We will represent it as an array $\mathbf{x} = (\mathbf{x}^a)$ or as the $n \times L$ tableau:

$$\mathbf{x} = (x_i^a) = \begin{pmatrix} x_1^n & \cdots & x_L^n \\ \vdots & \ddots & \vdots \\ x_1^1 & \cdots & x_L^1 \end{pmatrix},$$

which is conveniently depicted by a dot diagram. For instance when $(n, L) = (4, 3)$, it looks as

$$\mathbf{x} = \begin{pmatrix} 2 & 0 & 1 \\ 1 & 2 & 2 \\ 1 & 1 & 4 \\ 3 & 2 & 3 \end{pmatrix} = \begin{array}{|c|c|c|} \hline \bullet\bullet & & \bullet \\ \hline \bullet & \bullet\bullet & \bullet\bullet \\ \hline \bullet & \bullet & \bullet\bullet\bullet \\ \hline \bullet\bullet & \bullet\bullet & \bullet\bullet \\ \hline \end{array} \in B_8 \otimes B_6 \otimes B_5 \otimes B_3 = B(2, 1, 2, 3). \quad (3.5)$$

The dynamics of our n -line process will be described as a motion of dots. There is another multiline process relevant to the n -TASEP [8] which was reformulated in terms of crystals in [17]. The basic set there is $B^\ell = \{(x_1, \dots, x_L) \in \{0, 1\}^L \mid x_1 + \dots + x_L = \ell\}$ corresponding to the antisymmetric tensor representation instead of the B_ℓ in (3.2).

3.2. Auxiliary sets \mathcal{A} and \mathcal{B} . Let $[a, b]$ denote the set $\{a, a+1, \dots, b\}$ for the integers $a \leq b$. We set $(x)_+ = \max(x, 0)$ so that $(x)_+ - (-x)_+ = x$ holds.

Given an n -line state $\mathbf{x} \in B(\mathbf{m})$ we attach to it the sets $\mathcal{A}_{\mathbf{x}}$ and $\mathcal{B}_{\mathbf{x}}$ defined by

$$\mathcal{A}_{\mathbf{x}} = \{(i, a, k) \mid (i, a) \in \mathbb{Z}_L \times [1, n], 1 \leq k \leq (x_{i+1}^a - x_i^{a-1})_+\}, \quad (3.6)$$

$$\mathcal{B}_{\mathbf{x}} = \{(i, a, k) \mid (i, a) \in \mathbb{Z}_L \times [1, n], 1 \leq k \leq (x_i^a - x_{i+1}^{a+1})_+\}, \quad (3.7)$$

where the convention $x_i^0 = x_i^{n+1} = 0$ for all $i \in \mathbb{Z}_L$ should be applied throughout.

Example 3.1. For \mathbf{x} in (3.5) they read

$$\begin{aligned} \mathcal{A}_{\mathbf{x}} &= \{(1, 1, 1), (1, 1, 2), (1, 3, 1), (2, 1, 1), (2, 1, 2), (2, 1, 3), \\ &\quad (2, 2, 1), (2, 2, 2), (2, 3, 1), (3, 1, 1), (3, 1, 2), (3, 1, 3)\}, \\ \mathcal{B}_{\mathbf{x}} &= \{(1, 1, 1), (1, 1, 2), (1, 3, 1), (1, 4, 1), (1, 4, 2), (2, 3, 1), \\ &\quad (3, 1, 1), (3, 1, 2), (3, 2, 1), (3, 2, 2), (3, 2, 3), (3, 4, 1)\}. \end{aligned}$$

Example 3.2. Take

$$\mathbf{x} = \begin{pmatrix} 0 & 0 & 1 \\ 2 & 1 & 0 \\ 2 & 0 & 2 \\ 1 & 1 & 4 \end{pmatrix} \in B_6 \otimes B_4 \otimes B_3 \otimes B_1 = B(2, 1, 2, 1)$$

with $(n, L) = (4, 3)$. Then we have

$$\begin{aligned} \mathcal{A}_{\mathbf{x}} &= \{(1, 1, 1), (2, 1, 1), (2, 1, 2), (2, 1, 3), (2, 1, 4), (2, 2, 1), (3, 1, 1)\}, \\ \mathcal{B}_{\mathbf{x}} &= \{(1, 1, 1), (1, 2, 1), (1, 3, 1), (1, 3, 2), (3, 1, 1), (3, 1, 2), (3, 4, 1)\}. \end{aligned}$$

The coincidence of the cardinality of $\mathcal{A}_{\mathbf{x}}$ and $\mathcal{B}_{\mathbf{x}}$ in these example is not accidental.

Lemma 3.3. *For any $\mathbf{x} \in B(\mathbf{m})$, $\#\mathcal{A}_{\mathbf{x}} = \#\mathcal{B}_{\mathbf{x}}$ holds.*

Proof.

$$\begin{aligned}
\#\mathcal{A}_{\mathbf{x}} - \#\mathcal{B}_{\mathbf{x}} &= \sum_{i \in \mathbb{Z}_L} \sum_{a=1}^n (x_{i+1}^a - x_i^{a-1})_+ - \sum_{i \in \mathbb{Z}_L} \sum_{a=1}^n (x_i^a - x_{i+1}^{a+1})_+ \\
&= \sum_{i \in \mathbb{Z}_L} \sum_{a=0}^n \left((x_{i+1}^{a+1} - x_i^a)_+ - (x_i^a - x_{i+1}^{a+1})_+ \right) \\
&= \sum_{i \in \mathbb{Z}_L} \sum_{a=0}^n (x_{i+1}^{a+1} - x_i^a) = \sum_{i \in \mathbb{Z}_L} \sum_{a=0}^n (x_i^{a+1} - x_i^a) = \sum_{i \in \mathbb{Z}_L} (x_{i+1}^{n+1} - x_i^0) = 0.
\end{aligned}$$

□

We introduce the auxiliary sets \mathcal{A} and \mathcal{B} by

$$\begin{aligned}
\mathcal{A} &= \bigsqcup_{\mathbf{x} \in B(\mathbf{m})} \{\mathbf{x}\} \times \mathcal{A}_{\mathbf{x}} = \{(\mathbf{x}, (i, a, k)) \mid \mathbf{x} \in B(\mathbf{m}), (i, a, k) \in \mathcal{A}_{\mathbf{x}}\}, \\
\mathcal{B} &= \bigsqcup_{\mathbf{x} \in B(\mathbf{m})} \mathcal{B}_{\mathbf{x}} \times \{\mathbf{x}\} = \{((i, a, k), \mathbf{x}) \mid \mathbf{x} \in B(\mathbf{m}), (i, a, k) \in \mathcal{B}_{\mathbf{x}}\}.
\end{aligned}$$

The order of \mathbf{x} and (i, a, k) in the products is a matter of convention but taking them differently as above helps to distinguish \mathcal{A} and \mathcal{B} . By Lemma 3.3 we know $\#\mathcal{A} = \#\mathcal{B}$.

3.3. Bijection between \mathcal{A} and \mathcal{B} . Pick any $(\mathbf{x}, (i, a, k)) \in \mathcal{A}$. It implies $1 \leq k \leq x_{i+1}^a - x_i^{a-1}$, hence $x_i^{a-1} < x_{i+1}^a$ holds. Suppose that $x_i^{b-1} < x_{i+1}^b$ holds for $a \leq b \leq c$ until it ceases to do so at $b = c + 1$, namely $x_i^c \geq x_{i+1}^{c+1}$. Due to the convention $x_i^{n+1} = 0$, such $c \in [a, n]$ exists uniquely. We define the map T by

$$\begin{aligned}
T : \mathcal{A} &\rightarrow \mathcal{B}; \quad (\mathbf{x}, (i, a, k)) \mapsto ((i, c, l), \mathbf{y}), \\
\mathbf{y} = (y_j^b), \quad y_j^b &= x_j^b \quad \text{except} \quad (y_i^b, y_{i+1}^b) = \begin{cases} (x_i^b + x_{i+1}^b - x_i^{b-1}, x_i^{b-1}) & \text{if } b \in [a+1, c], \\ (x_i^a + k, x_{i+1}^a - k) & \text{if } b = a, \end{cases} \quad (3.8) \\
l &= \begin{cases} k & \text{if } c = a, \\ x_{i+1}^c - x_i^{c-1} & \text{if } c > a. \end{cases}
\end{aligned}$$

When $c = a$, the case $b \in [a+1, c]$ can just be omitted. It is easy to see $T\mathcal{A} \subseteq \mathcal{B}$. In fact from (3.7) and (3.8) it suffices to check $y_i^b \geq 0$ ($b \in [a+1, c]$), $y_{i+1}^a \geq 0$ and $1 \leq l \leq y_i^c - y_{i+1}^{c+1}$. They all follow from the definition straightforwardly.

Similarly pick any $((i, a, k), \mathbf{x}) \in \mathcal{B}$. It implies $1 \leq k \leq x_i^a - x_{i+1}^{a+1}$ hence $x_i^a > x_{i+1}^{a+1}$ holds. Suppose that $x_i^b > x_{i+1}^{b+1}$ holds for $d \leq b \leq a$ until it ceases to do so at $b = d - 1$, namely $x_i^{d-1} \leq x_{i+1}^d$. Due to the convention $x_i^0 = 0$, such $d \in [1, a]$ exists uniquely. We define the map S by

$$\begin{aligned}
S : \mathcal{B} &\rightarrow \mathcal{A}; \quad ((i, a, k), \mathbf{x}) \mapsto (\mathbf{y}, (i, d, m)), \\
\mathbf{y} = (y_j^b), \quad y_j^b &= x_j^b \quad \text{except} \quad (y_i^b, y_{i+1}^b) = \begin{cases} (x_i^a - k, x_{i+1}^a + k) & b = a, \\ (x_{i+1}^{b+1}, x_i^b + x_{i+1}^b - x_{i+1}^{b+1}) & b \in [d, a-1], \end{cases} \quad (3.9) \\
m &= \begin{cases} k & \text{if } d = a, \\ x_i^d - x_{i+1}^{d+1} & \text{if } d < a. \end{cases}
\end{aligned}$$

When $d = a$, the case $b \in [d, a-1]$ can just be omitted. Again $S\mathcal{B} \subseteq \mathcal{A}$ is easily seen.

Focusing on the i -th and the $(i + 1)$ -th columns of the tableaux \mathbf{x} and \mathbf{y} , we set $(\alpha_b, \beta_b) = (x_i^b, x_{i+1}^b)$ for simplicity. Then their nontrivial changes in (3.8) and (3.9) look as follows:

$$\begin{array}{ccc}
\begin{array}{c} x_i^b \quad x_{i+1}^b \\ \left| \begin{array}{c|c} \alpha_{c+1} & \beta_{c+1} \\ \alpha_c & \beta_c \\ \vdots & \vdots \\ \alpha_{a+1} & \beta_{a+1} \\ \alpha_a & \beta_a \\ \alpha_{a-1} & \beta_{a-1} \end{array} \right| \end{array} & \xrightarrow{T} & \begin{array}{c} y_i^b \quad y_{i+1}^b \\ \left| \begin{array}{c|c} \alpha_{c+1} & \beta_{c+1} \\ * & \alpha_{c-1} \\ \vdots & \vdots \\ * & \alpha_a \\ * & \beta_{a-k} \\ \alpha_{a-1} & \beta_{a-1} \end{array} \right| \end{array} & \begin{array}{c} x_i^b \quad x_{i+1}^b \\ \left| \begin{array}{c|c} \alpha_{a+1} & \beta_{a+1} \\ \alpha_a & \beta_a \\ \alpha_{a-1} & \beta_{a-1} \\ \vdots & \vdots \\ \alpha_d & \beta_d \\ \alpha_{d-1} & \beta_{d-1} \end{array} \right| \end{array} & \xrightarrow{S} & \begin{array}{c} y_i^b \quad y_{i+1}^b \\ \left| \begin{array}{c|c} \alpha_{a+1} & \beta_{a+1} \\ \alpha_{a-k} & * \\ \beta_a & * \\ \vdots & \vdots \\ \beta_{d+1} & * \\ \alpha_{d-1} & \beta_{d-1} \end{array} \right| \end{array} \\
\text{(i)} & & \text{(ii)} & \text{(iii)} & \text{(iv)} & \text{(3.10)}
\end{array}$$

Here $*$ signifies the integers so chosen that the sum is conserved in each row. It implies that the dots in the diagram like (3.5) always move horizontally to the left (resp. right) neighbor slot by T (resp. S).

Proposition 3.4. T and S are bijections satisfying $TS = \text{id}_{\mathcal{B}}$ and $ST = \text{id}_{\mathcal{A}}$.

Proof. Thanks to Lemma 3.3 it suffices to prove $ST = \text{id}_{\mathcal{A}}$. Let $T : (\mathbf{x}, (i, a, k)) \mapsto ((i, c, l), \mathbf{y})$. The right hand side is depicted in (ii) of (3.10) and we have already seen that it belongs to \mathcal{B} after (3.8). First we show that (ii) satisfies the inequalities in (iii) $_{(a,d) \rightarrow (c,a)}$. In fact the bottom one $\beta_a - k \geq \alpha_{a-1}$, for example, follows from the condition $(i, a, k) \in \mathcal{A}_{\mathbf{x}}$ (3.6). The rest are similar. Now we can inscribe the same numbers as (ii) into (iii) $_{(a,d) \rightarrow (c,a)}$. Then the rule (iii) \mapsto (iv) reproduces \mathbf{x} . Second we check that m given in (3.9) returns to the original value k when applied to (ii). For $d = a$ this is obvious. For $d < a$ we have $m = (\text{bottom } * \text{ in (ii)}) - \alpha_a = (\alpha_a + k) - \alpha_a = k$ as desired. Thus ST reproduces (i, a, k) as well as \mathbf{x} . \square

Example 3.5. For \mathbf{x} and $(i, a, k) \in \mathcal{A}_{\mathbf{x}}$ in Example 3.2, the image of $(\mathbf{x}, (i, a, k))$ under T reads

$$\begin{aligned}
(\mathbf{x}, (1, 1, 1)) &\mapsto \left((1, 1, 1), \begin{pmatrix} 0 & 0 & 1 \\ 2 & 1 & 0 \\ 2 & 0 & 2 \\ 2 & 0 & 4 \end{pmatrix} \right), & (\mathbf{x}, (2, 1, 1)) &\mapsto \left((2, 2, 1), \begin{pmatrix} 0 & 0 & 1 \\ 2 & 1 & 0 \\ 2 & 1 & 1 \\ 1 & 2 & 3 \end{pmatrix} \right), \\
(\mathbf{x}, (2, 1, 2)) &\mapsto \left((2, 2, 1), \begin{pmatrix} 0 & 0 & 1 \\ 2 & 1 & 0 \\ 2 & 1 & 1 \\ 1 & 3 & 2 \end{pmatrix} \right), & (\mathbf{x}, (2, 1, 3)) &\mapsto \left((2, 2, 1), \begin{pmatrix} 0 & 0 & 1 \\ 2 & 1 & 0 \\ 2 & 1 & 1 \\ 1 & 4 & 1 \end{pmatrix} \right), \\
(\mathbf{x}, (2, 1, 4)) &\mapsto \left((2, 2, 1), \begin{pmatrix} 0 & 0 & 1 \\ 2 & 1 & 0 \\ 2 & 1 & 1 \\ 1 & 5 & 0 \end{pmatrix} \right), & (\mathbf{x}, (2, 2, 1)) &\mapsto \left((2, 2, 1), \begin{pmatrix} 0 & 0 & 1 \\ 2 & 1 & 0 \\ 2 & 1 & 1 \\ 1 & 1 & 4 \end{pmatrix} \right), \\
(\mathbf{x}, (3, 1, 1)) &\mapsto \left((3, 1, 1), \begin{pmatrix} 0 & 0 & 1 \\ 2 & 1 & 0 \\ 2 & 0 & 2 \\ 0 & 1 & 5 \end{pmatrix} \right).
\end{aligned}$$

Reversing these arrows provides examples of the image under S .

3.4. Stochastic dynamics. In the transformation $T : (\mathbf{x}, (i, a, k)) \mapsto ((i, c, l), \mathbf{y})$ in (3.8), we write the uniquely determined element $\mathbf{y} \in B(\mathbf{m})$ as $\mathbf{y} = T_{i,a}^k(\mathbf{x})$. In this way we have the

deterministic evolution $T_{i,a}^k$ on $B(\mathbf{m})$ such that

$$T : (\mathbf{x}, (i, a, k)) \mapsto ((i, c, l), T_{i,a}^k(\mathbf{x})). \quad (3.11)$$

It is defined for each $(i, a, k) \in \mathcal{A}_{\mathbf{x}}$. For a later convenience we also set

$$T_{i,a}^k(\mathbf{x}) = \mathbf{x} \quad \text{if } (i, a, k) \notin \mathcal{A}_{\mathbf{x}}. \quad (3.12)$$

Given $\mathbf{x} = (x_i^a) \in B(\mathbf{m})$, suppose that $t := x_{i+1}^a - x_i^{a-1} \geq 1$ so that $\mathcal{A}_{\mathbf{x}}$ (3.6) contains $(i, a, 1), (i, a, 2), \dots, (i, a, t)$. Then it is easy to see $T_{i,a}^k(\mathbf{x}) = (T_{i,a}^1)^k(\mathbf{x})$ for $k \in [1, t]$.

By the n -line process with prescribed multiplicity \mathbf{m} , we mean the stochastic process on $B(\mathbf{m})$ in which each state $\mathbf{x} \in B(\mathbf{m})$ undergoes the time evolution $T_{i,a}^k$ with an equal transition rate for all $(i, a, k) \in \mathcal{A}_{\mathbf{x}}$. Let $\bigoplus_{\mathbf{x} \in B(\mathbf{m})} \mathbb{C}|\mathbf{x}\rangle$ be its space of states having the basis $\{|\mathbf{x}\rangle\}$ labeled with $\mathbf{x} = (x_i^a) \in B(\mathbf{m})$ (3.4). By the definition, the Markov matrix of the n -line process (LP) reads as

$$H_{\text{LP}} = \sum_{i \in \mathbb{Z}_L} \sum_{a=1}^n \sum_{k \geq 1} (T_{i,a}^k - 1), \quad (3.13)$$

which is convergent owing to (3.12).

3.5. Steady state. The n -line process on $B(\mathbf{m})$ possesses a unique steady state. Let $\mu(\mathbf{x})$ denote its probability distribution.

Theorem 3.6. *The stationary probability distribution of the n -line process is uniform. Namely $\mu(\mathbf{x})$ is independent of $\mathbf{x} \in B(\mathbf{m})$.*

Proof. Since the steady state is unique, it suffices to show that the total rate P_{in} jumping into a given state \mathbf{x} is equal to the total rate P_{out} jumping out of it under the uniform choice $\mu(\mathbf{x}) = \mu$. One has $P_{\text{out}} = (\#\mathcal{A}_{\mathbf{x}})\mu(\mathbf{x}) = (\#\mathcal{A}_{\mathbf{x}})\mu$. On the other hand, P_{in} is calculated as

$$\begin{aligned} P_{\text{in}} &= \sum_{\mathbf{y} \in B(\mathbf{m})} \sum_{(i,a,k) \in \mathcal{A}_{\mathbf{y}}} \theta(T_{i,a}^k(\mathbf{y}) = \mathbf{x})\mu(\mathbf{y}) \\ &= \mu \sum_{(\mathbf{y}, (i,a,k)) \in \mathcal{A}} \sum_{(j,b,l) \in \mathcal{B}_{\mathbf{x}}} \theta(T : (\mathbf{y}, (i, a, k)) \mapsto ((j, b, l), \mathbf{x})) \\ &= \mu \sum_{(j,b,l) \in \mathcal{B}_{\mathbf{x}}} \sum_{(\mathbf{y}, (i,a,k)) \in \mathcal{A}} \theta(S : ((j, b, l), \mathbf{x}) \mapsto (\mathbf{y}, (i, a, k))) \\ &= \mu \sum_{(j,b,l) \in \mathcal{B}_{\mathbf{x}}} 1 = (\#\mathcal{B}_{\mathbf{x}})\mu = (\#\mathcal{A}_{\mathbf{x}})\mu, \end{aligned}$$

where the last equality is due to Lemma 3.3. \square

We summarize the result as

Corollary 3.7 (Steady state of n -line process).

$$H_{\text{LP}}|\Omega(\mathbf{m})\rangle = 0, \quad |\Omega(\mathbf{m})\rangle = \sum_{\mathbf{x} \in B(\mathbf{m})} |\mathbf{x}\rangle.$$

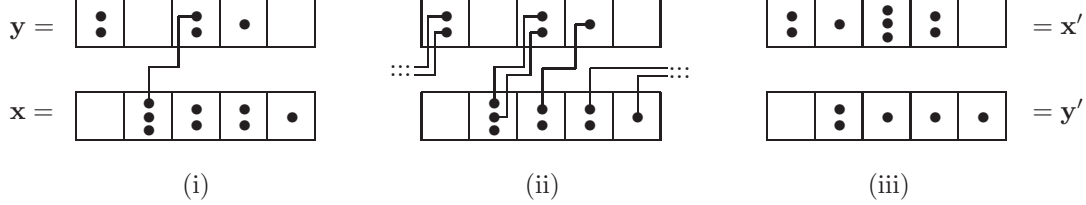
4. PROJECTION FROM n -LINE PROCESS TO n -TAZRP

4.1. Combinatorial R . The B_ℓ defined in (3.2) is a labeling set of a basis of the ℓ -fold symmetric tensor representation of the quantum affine algebra $U_q(\widehat{sl}_L)$ [5, 12]. The *combinatorial R* is the quantum R matrix at $q = 0$. It is a bijection

$$R = R_{\ell,m} : B_\ell \otimes B_m \rightarrow B_m \otimes B_\ell; \quad \mathbf{x} \otimes \mathbf{y} \mapsto \mathbf{y}' \otimes \mathbf{x}'. \quad (4.1)$$

To describe it explicitly we set $\mathbf{x} = (x_1, \dots, x_L), \mathbf{y} = (y_1, \dots, y_L), \mathbf{x}' = (x'_1, \dots, x'_L)$ and $\mathbf{y}' = (y'_1, \dots, y'_L)$. Note that $\sum_i x_i = \sum_i x'_i = \ell$ and $\sum_i y_i = \sum_i y'_i = m$. Given $\mathbf{x} = (0, 3, 2, 2, 1)$ and $\mathbf{y} = (2, 0, 2, 1, 0)$ for instance, we depict them as the diagram (i) given below. In this paper we

will only encounter the case $\ell > m$. Then the algorithm [21, Rule 3.11] known as the *NY-rule* for finding \mathbf{x}' and \mathbf{y}' goes as follows:



- (i) Choose a dot, say d , in \mathbf{y} and connect it to a dot d' in \mathbf{x} to form a pair. d' should be the rightmost one among those located strictly left of d . If there is no such dot, take d' to be the rightmost one in \mathbf{x} , i.e., seek such d' under the *periodic boundary condition*. (Dots in the same box are regarded to be in the same position. If d' is to be chosen from more than one dots in a box, any of them can be taken.)
- (ii) Repeat (i) for yet unpaired dots until all dots in \mathbf{y} are paired to some dots in \mathbf{x} .
- (iii) Move the $\ell - m$ unpaired dots in \mathbf{x} vertically up to \mathbf{y} . The resulting diagrams give \mathbf{x}' and \mathbf{y}' .

In the above example we have $\mathbf{x}' = (2, 1, 3, 2, 0)$ and $\mathbf{y}' = (0, 2, 1, 1, 1)$. The lines pairing the dots are called *H-lines*². We note that the NY-rule implies

$$R(\mathbf{x} \otimes \mathbf{y}) = \mathbf{y}' \otimes \mathbf{x}' \in B_m \otimes B_\ell \implies \mathbf{x} \geq \mathbf{y}', \mathbf{x}' \geq \mathbf{y} \quad (4.2)$$

for $\ell > m$, where in general for $\mathbf{u} = (u_1, \dots, u_L), \mathbf{v} = (v_1, \dots, v_L) \in \mathbb{Z}^L$, $\mathbf{u} \geq \mathbf{v}$ is defined by $\mathbf{u} - \mathbf{v} \in (\mathbb{Z}_{\geq 0})^L$.

Remark 4.1.

- (1) In (i) and (ii), the *H-lines* depend on the order of choosing dots from \mathbf{y} . However the final result \mathbf{x}' and \mathbf{y}' are independent of it due to [21, Prop.3.20].
- (2) A similar algorithm is known for the case $\ell < m$. $R_{\ell, m}$ is identity for $\ell = m$. In any case $R_{\ell, m} R_{m, \ell} = \text{id}_{B_m \otimes B_\ell}$ holds.
- (3) The above rule is close to but slightly different from the combinatorial R of the *antisymmetric* tensor representation which was identified [17] with the arrival/service/departure process relevant to TASEP [8]. In this interpretation one regards that time increases horizontally to the left (apart from the periodic boundary condition). Then the customers (dots in \mathbf{y}) in the present case have to avoid the service (dots in \mathbf{x}) that becomes available simultaneously with their arrival. Another significant difference is, there can be *multiple* arrival and service at a time reflecting the symmetric tensor representation.
- (4) The following explicit formula having background in geometric crystals and soliton cellular automata [11] is known to hold either for $\ell \geq m$ or $\ell \leq m$ [24]:

$$x'_i = x_i + Q_i(x, y) - Q_{i-1}(x, y), \quad y'_i = y_i + Q_{i-1}(x, y) - Q_i(x, y) \quad (i \in \mathbb{Z}_L),$$

$$Q_i(x, y) = \min \left\{ \sum_{j=1}^{k-1} x_{i+j} + \sum_{j=k+1}^L y_{i+j} \mid 1 \leq k \leq L \right\}.$$

It is customary to depict the relation (4.1) as a vertex:

$$\begin{array}{ccc} & \mathbf{y}' & \\ & \uparrow & \\ \mathbf{x} & \text{---} & \mathbf{x}' \\ & \downarrow & \\ & \mathbf{y} & \end{array} \quad (4.3)$$

² The nomenclature *H* originates in [4, (2.5)] and [15, (1.1.3)] etc., which has the meaning of *local Hamiltonian* of corner transfer matrices [1].

One may rotate it arbitrarily. The thick arrows here carry crystals B_ℓ or B_m . They are to be distinguished from the thin arrows carrying a Fock space F which will be used in Section 5.2 and 5.3.

The most significant property of the combinatorial R is the Yang-Baxter equation [1]:

$$(R \otimes 1)(1 \otimes R)(R \otimes 1) = (1 \otimes R)(R \otimes 1)(1 \otimes R)$$

as maps $B_\ell \otimes B_m \otimes B_k \rightarrow B_k \otimes B_m \otimes B_\ell$ for any ℓ, m, k . For example the two sides acting on the element $0121 \otimes 1101 \otimes 2000 \in B_4 \otimes B_3 \otimes B_2$ lead to³

$$\begin{array}{ccccc}
 0011 & 0111 & 3100 & & 0011 & 0111 & 3100 \\
 \swarrow \nearrow & & \uparrow & & \uparrow & \swarrow \nearrow & \\
 0021 & 0101 & 3100 & = & 0011 & 0211 & 3000 \\
 \uparrow & \swarrow \nearrow & & & \swarrow \nearrow & & \uparrow \\
 0021 & 1201 & 2000 & & 0121 & 0101 & 3000 \\
 \swarrow \nearrow & & \uparrow & & \uparrow & \swarrow \nearrow & \\
 0121 & 1101 & 2000 & & 0121 & 1101 & 2000
 \end{array} \tag{4.4}$$

Here = means that starting from the same bottom line one ends up with the same top line. In this way one can move the arrows across other vertices without changing outer states. This property will be utilized efficiently in the sequel.

Combinatorial R 's form the most systematic examples of the set theoretical solutions to the Yang-Baxter equation [6, 23] connected to the representation theory of quantum groups, which have numerous applications [9, 11, 15, 16, 21, 24].

4.2. $B_+(\mathbf{m})$ and elementary bijection φ . Recall that the sets of configurations are given by $B(\mathbf{m})$ (3.2) for n -line process and by $S(\mathbf{m})$ (2.5) for n -TAZRP. We introduce a subsidiary set

$$B_+(\mathbf{m}) = \{\mathbf{x}^1 \otimes \cdots \otimes \mathbf{x}^n \in B(\mathbf{m}) \mid \mathbf{x}^1 \geq \cdots \geq \mathbf{x}^n\} \subseteq B(\mathbf{m}),$$

where \geq is defined after (4.2). There is an elementary bijection between $B_+(\mathbf{m})$ and $S(\mathbf{m})$ as

$$\begin{aligned}
 \varphi : S(\mathbf{m}) &\xrightarrow{\sim} B_+(\mathbf{m}); & \sigma = (\sigma_i^a) &\mapsto \varphi^1(\sigma) \otimes \cdots \otimes \varphi^n(\sigma), \\
 \varphi^a(\sigma) &= (\sigma_1^a + \sigma_1^{a+1} + \cdots + \sigma_1^n, \dots, \sigma_L^a + \sigma_L^{a+1} + \cdots + \sigma_L^n),
 \end{aligned} \tag{4.5}$$

where $\varphi^a(\sigma) \in B_{\ell_a}$ and $\varphi^1(\sigma) \geq \cdots \geq \varphi^n(\sigma)$ are obvious.

Example 4.2. The $\varphi^1(\sigma), \dots, \varphi^n(\sigma)$ are easily read off from the dot diagram (see (3.5)) by regarding a particle of species a as a column of a dots filled from the bottom. The following is an example for $(n, L) = (3, 4)$, giving $\varphi^1(\sigma) = 1213 \in B_7$, $\varphi^2(\sigma) = 1201 \in B_4$ and $\varphi^3(\sigma) = 0101 \in B_2$.

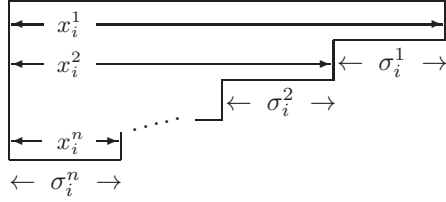
multiplicity rep.	multiset rep.	$\varphi^3(\sigma) =$	<table style="border-collapse: collapse; text-align: center;"> <tr><td style="width: 20px; height: 20px;"></td><td style="width: 20px; height: 20px;">•</td><td style="width: 20px; height: 20px;"></td><td style="width: 20px; height: 20px;">•</td></tr> <tr><td style="width: 20px; height: 20px;"></td><td style="width: 20px; height: 20px;">••</td><td style="width: 20px; height: 20px;"></td><td style="width: 20px; height: 20px;">•</td></tr> <tr><td style="width: 20px; height: 20px;">•</td><td style="width: 20px; height: 20px;">••</td><td style="width: 20px; height: 20px;">•</td><td style="width: 20px; height: 20px;">•••</td></tr> </table>		•		•		••		•	•	••	•	•••
	•		•												
	••		•												
•	••	•	•••												
$\sigma = (010, 011, 100, 201) = (2, 23, 1, 113)$		$\varphi^2(\sigma) =$	<table style="border-collapse: collapse; text-align: center;"> <tr><td style="width: 20px; height: 20px;">•</td><td style="width: 20px; height: 20px;">••</td><td style="width: 20px; height: 20px;"></td><td style="width: 20px; height: 20px;">•</td></tr> <tr><td style="width: 20px; height: 20px;">•</td><td style="width: 20px; height: 20px;">••</td><td style="width: 20px; height: 20px;">•</td><td style="width: 20px; height: 20px;">•••</td></tr> </table>	•	••		•	•	••	•	•••				
•	••		•												
•	••	•	•••												
$\varphi(\sigma) = 1213 \otimes 1201 \otimes 0101$		$\varphi^1(\sigma) =$	<table style="border-collapse: collapse; text-align: center;"> <tr><td style="width: 20px; height: 20px;">•</td><td style="width: 20px; height: 20px;">••</td><td style="width: 20px; height: 20px;">•</td><td style="width: 20px; height: 20px;">•••</td></tr> </table>	•	••	•	•••								
•	••	•	•••												
			<table style="border-collapse: collapse; margin: 0 auto;"> <tr><td style="padding: 0 10px;">2</td><td style="padding: 0 10px;">23</td><td style="padding: 0 10px;">1</td><td style="padding: 0 10px;">113</td></tr> </table>	2	23	1	113								
2	23	1	113												

The inverse of φ is given by

$$\begin{aligned}
 \varphi^{-1} : B_+(\mathbf{m}) &\xrightarrow{\sim} S(\mathbf{m}); & \mathbf{x} = (x_i^a) &\mapsto (\sigma_i^a), \\
 \sigma_i^a &= x_i^a - x_i^{a+1} & (x_i^{n+1} &= 0).
 \end{aligned} \tag{4.6}$$

³ $(0, 1, 2, 1)$ for example is denoted by 0121 for simplicity. A similar convention will also be used in the rest of the paper.

See Section 3.1. The maps $\varphi^{\pm 1}$ are also simply seen by the following diagram for each $i \in \mathbb{Z}_L$:



In this Young diagram for site i , a particle with species a corresponds to a column of depth a .

4.3. Projection π . We are going to construct a map $\pi : B(\mathbf{m}) \rightarrow S(\mathbf{m})$ as the composition of maps

$$\begin{array}{ccccc} B(\mathbf{m}) & \xrightarrow{\pi^1 \otimes \cdots \otimes \pi^n} & B_+(\mathbf{m}) & \xrightarrow{\varphi^{-1}} & S(\mathbf{m}) \\ \mathbf{x} & \mapsto & \pi^1(\mathbf{x}) \otimes \cdots \otimes \pi^n(\mathbf{x}) & \mapsto & \boldsymbol{\sigma} = (\sigma_1, \dots, \sigma_L), \end{array} \quad (4.7)$$

where φ^{-1} is given by (4.6). Thus the remaining task is to construct

$$\pi^a : B(\mathbf{m}) = B_{\ell_1} \otimes \cdots \otimes B_{\ell_n} \rightarrow B_{\ell_a}; \quad \mathbf{x} = \mathbf{x}^1 \otimes \cdots \otimes \mathbf{x}^n \mapsto \pi^a(\mathbf{x})$$

for each $a \in [1, n]$. For $a = 1$ we set $\pi^1(\mathbf{x}) = \mathbf{x}^1$. For $a \in [2, n]$ we set

$$R^1 \cdots R^{a-2} R^{a-1}(\mathbf{x}^1 \otimes \cdots \otimes \mathbf{x}^a) = \pi^a(\mathbf{x}) \otimes \mathbf{u}^1 \otimes \cdots \otimes \mathbf{u}^{a-1}, \quad (4.8)$$

where R^b is the combinatorial R acting on the $(b, b+1)$ -th components from the left. The product $R^1 \cdots R^{a-1}$ lets B_{ℓ_a} penetrate through $B_{\ell_1} \otimes \cdots \otimes B_{\ell_{a-1}}$ bringing it to the left end of the tensor product. The $\mathbf{u}^1 \otimes \cdots \otimes \mathbf{u}^{a-1} \in B_{\ell_1} \otimes \cdots \otimes B_{\ell_{a-1}}$ denotes the element thereby produced, which will not be used in the sequel. The $\pi^a(\mathbf{x})$ is depicted for $a = 1, 2, 3$ as

$$\begin{array}{ccc} \pi^1(\mathbf{x}) \leftarrow \mathbf{x}^1 & \pi^2(\mathbf{x}) \leftarrow \begin{array}{c} \uparrow \mathbf{u}^1 \\ \mathbf{x}^2 \\ \downarrow \mathbf{x}^1 \end{array} & \pi^3(\mathbf{x}) \leftarrow \begin{array}{cc} \uparrow \mathbf{u}^1 & \uparrow \mathbf{u}^2 \\ \mathbf{x}^3 \\ \downarrow \mathbf{x}^1 & \downarrow \mathbf{x}^2 \end{array} \end{array} \quad (4.9)$$

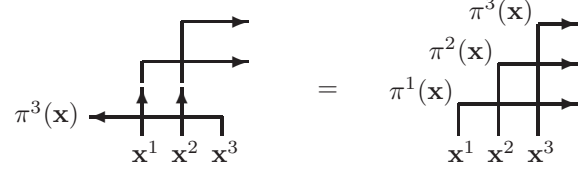
The diagram for $\pi^3(\mathbf{x})$ is a concatenation of (4.3) rotated by 90 degrees. Note that $\pi^a(\mathbf{x})$ actually depends only on the left a components of $\mathbf{x} = \mathbf{x}^1 \otimes \cdots \otimes \mathbf{x}^n$. We postpone the proof of the fact $\pi^1(\mathbf{x}) \otimes \cdots \otimes \pi^n(\mathbf{x}) \in B_+(\mathbf{m})$ to Lemma 4.4.

Example 4.3. Consider $\mathbf{x} = 114 \otimes 202 \otimes 210 \otimes 001$ in Example 3.2. Then $\pi^1(\mathbf{x}) = 114$ and the other $\pi^a(\mathbf{x})$'s are determined from the diagrams

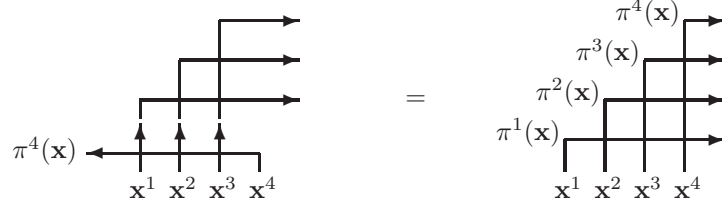
$$\begin{array}{ccc} \begin{array}{c} 204 \\ \uparrow \\ 112 \leftarrow \mathbf{x}^2 \\ \downarrow \\ 114 \end{array} & \begin{array}{cc} \begin{array}{c} 105 \\ \uparrow \\ 111 \leftarrow \mathbf{x}^2 \\ \downarrow \\ 114 \end{array} & \begin{array}{c} 310 \\ \uparrow \\ 102 \leftarrow \mathbf{x}^2 \\ \downarrow \\ 202 \end{array} \end{array} & \begin{array}{ccc} \begin{array}{c} 213 \\ \uparrow \\ 001 \leftarrow \mathbf{x}^2 \\ \downarrow \\ 114 \end{array} & \begin{array}{c} 112 \\ \uparrow \\ 100 \leftarrow \mathbf{x}^2 \\ \downarrow \\ 202 \end{array} & \begin{array}{c} 201 \\ \uparrow \\ 010 \leftarrow \mathbf{x}^2 \\ \downarrow \\ 210 \end{array} \end{array} \end{array}$$

as $\pi^2(\mathbf{x}) = 112$, $\pi^3(\mathbf{x}) = 111$ and $\pi^4(\mathbf{x}) = 001$. They indeed satisfy $\pi^1(\mathbf{x}) \geq \pi^2(\mathbf{x}) \geq \pi^3(\mathbf{x}) \geq \pi^4(\mathbf{x})$, assuring $\pi^1(\mathbf{x}) \otimes \pi^2(\mathbf{x}) \otimes \pi^3(\mathbf{x}) \otimes \pi^4(\mathbf{x}) \in B_+(\mathbf{m})$. Applying the bijection φ^{-1} (4.6) further we obtain the 4-TAZRP state $\pi(\mathbf{x}) = (3, 3, 1124)$ in multiset representation and $(0010, 0010, 2101)$ in multiplicity representation.

One can construct a *single* diagram that depicts $\pi^1(\mathbf{x}), \dots, \pi^n(\mathbf{x})$ simultaneously. We illustrate the procedure for $n = 3$.



First we attach an extra vertex on top of the defining diagram of $\pi^3(\mathbf{x})$. This enables us to apply the Yang-Baxter equation to move the arrow going from \mathbf{x}^3 to $\pi^3(\mathbf{x})$ around to get the right diagram, where the newly generated states on the diagonal boundary edges are identified with $\pi^1(\mathbf{x})$ and $\pi^2(\mathbf{x})$ by (4.9). A similar procedure for $n = 4$ goes as



Here we have used the diagram representation of $\pi^3(\mathbf{x})$ derived for $n = 3$. For n general it look as



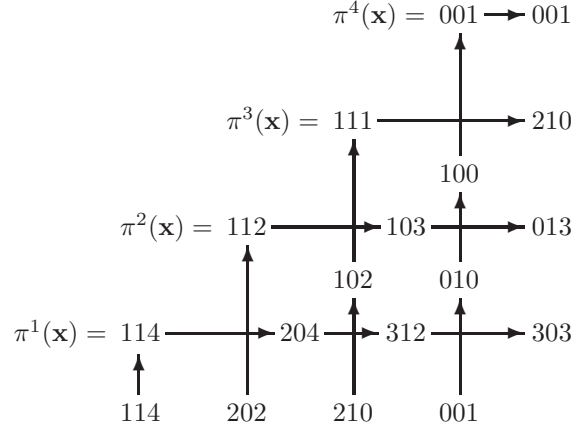
We have bent the arrows so that there are n incoming ones from the bottom and n outgoing ones to the right. This turns out to be a natural shape when the diagram is embedded into a layer-to-layer transfer matrix of 3D lattice model associated with the tetrahedron equation [18, 19]. Now we are ready to show that $\pi^1(\mathbf{x}) \otimes \dots \otimes \pi^n(\mathbf{x}) \in B_+(\mathbf{m})$ indeed holds in (4.7).

Lemma 4.4. $\pi^a(\mathbf{x})$ defined by (4.8) satisfies $\pi^1(\mathbf{x}) \geq \dots \geq \pi^n(\mathbf{x})$.

Proof. The diagram (4.10) tells that $R_{\ell_a, \ell_{a+1}}(\pi^a(\mathbf{x}) \otimes \mathbf{u}) = \pi^{a+1}(\mathbf{x}) \otimes \mathbf{v}$ holds for some $\mathbf{u} \in B_{\ell_{a+1}}$ and $\mathbf{v} \in B_{\ell_a}$. Then the assertion follows from (4.2). \square

The diagram (4.10) reminds us of a corner transfer matrix [1, Chap.13]. In fact, in the forthcoming Theorem 5.2 it will be used exactly as the matrix element of it for the $U_q(\widehat{sl}_L)$ -vertex model associated with the symmetric tensor representations of degrees $\ell_1, \ell_2, \dots, \ell_n$ at $q = 0$, where every vertex is frozen to the combinatorial R and all the edge variables are uniquely determined from the input $\mathbf{x}^1, \mathbf{x}^2, \dots, \mathbf{x}^n$.

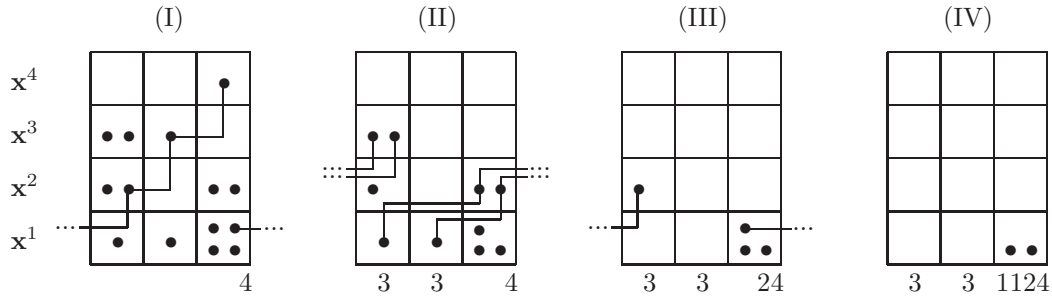
Example 4.5. Take again $\mathbf{x} = 114 \otimes 202 \otimes 210 \otimes 001$ in Example 3.2. Then $\pi^1(\mathbf{x}), \dots, \pi^4(\mathbf{x})$ are calculated as



They agree with those obtained in Example 4.3.

4.4. Queueing type algorithm for π and TAZRP embedding. Here we explain more human-friendly perceivable algorithm to derive the n -TAZRP state $\pi(\mathbf{x}) \in S(\mathbf{m})$ in multiset representation from an n -line state $\mathbf{x} = \mathbf{x}^1 \otimes \dots \otimes \mathbf{x}^n \in B(\mathbf{m})$. We illustrate it along the same example $\mathbf{x} = 114 \otimes 202 \otimes 210 \otimes 001$ and $\pi(\mathbf{x}) = (3, 3, 1124)$ with $(n, L) = (4, 3)$ as Example 3.2 and 4.3.

First draw the dot diagram (I) of $\mathbf{x} = \mathbf{x}^1 \otimes \dots \otimes \mathbf{x}^n$ as in (3.5).



Do the following procedure for $a = n, n - 1, \dots, 1$ in this order.

Draw an H -line from each dot in \mathbf{x}^a by applying the NY-rule repeatedly until it reaches some dot in the bottom row which belongs to \mathbf{x}^1 . Record the captured dots in \mathbf{x}^1 as particle of species a and erase all the dots connected by the H -lines.

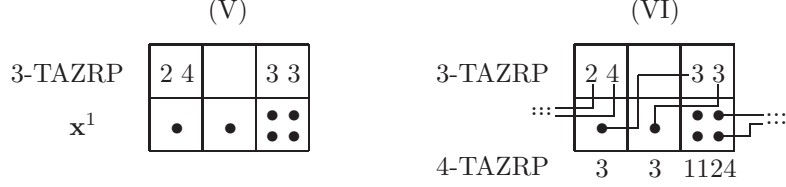
The array of multiset of particles gives the n -TAZRP configuration, i.e., the image of π .

For the procedure with $a = 1$, no H -line needs to be drawn and one just assigns 1 to the existing dots. For each a , the H -lines depend on the order of picking the dots in \mathbf{x}^a but the final output of the procedure does not depend on it thanks to Remark 4.1 (1). In the present example, one gets (I) \rightarrow (II) \rightarrow (III) \rightarrow (IV) as the procedure is executed for $a = 4, 3, 2, 1$. (We omitted the empty diagram produced by the last $a = 1$ case.)

The equivalence of the above algorithm for π and the definition (4.7) is shown easily if one notices that the composition of the combinatorial R to get $\pi^a(\mathbf{x})$ as in Example 4.3 is described as a repeated application of the NY-rule in a dot diagram.

One can further reformulate the algorithm inductively with respect to n so as to produce n -TAZRP states from $(n - 1)$ -TAZRP states and B_{ℓ_1} . Consider the above example for $n = 4$. The $\mathbf{x}^2 \otimes \mathbf{x}^3 \otimes \mathbf{x}^4$ without the bottom row \mathbf{x}^1 is an 3-line state whose projection is the 3-TAZRP state

(13, \emptyset , 22). Increase the species uniformly by 1 to get (24, \emptyset , 33)⁴ and (V) below.



Regard the 3-TAZRP state as a collection of particles with species $a = 2, 3, \dots, n$ ($n = 4$ in our ongoing illustration). Draw H -lines from them to the dots in \mathbf{x}^1 in the order $a = n, n-1, \dots, 2$ according to the NY-rule. For each a , the set of dots linked with the particles of species a is independent of the order of picking the particles due to Remark 4.1 (1). Regard the dots in $\mathbf{x}^1 \in B_{\ell_1}$ connected to the particles a also as particles a . Dots in $\mathbf{x}^1 \in B_{\ell_1}$ not captured by any H -line is regard as particle 1. Then the bottom row gives the n -TAZRP state. See (VI). In general the procedure (V) \rightarrow (VI) to get n -TAZRP states from B_{ℓ_1} and $(n-1)$ -TAZRP states (with species from $[2, n]$) is a modification of the NY-rule in that the one set of the dots is assigned with species and larger species ones have the priority to emanate an H -line. We call it the *TAZRP embedding rule*. For n -line states $\mathbf{x} = \mathbf{x}^1 \otimes \dots \otimes \mathbf{x}^n \in B(\mathbf{m})$, set

$$\begin{aligned} \{(k-1)\text{-TAZRP states}\} \times B_{\ell_{n-k+1}} &\longrightarrow \{k\text{-TAZRP states}\} \\ (\boldsymbol{\sigma}, \mathbf{x}^{n-k+1}) &\longmapsto \Phi_{k, \mathbf{x}^{n-k+1}}(\boldsymbol{\sigma}) \quad (k \in [2, n]). \end{aligned}$$

Here $\Phi_{k, \mathbf{x}^{n-k+1}}$ signifies the TAZRP embedding rule; one increases the species of particles in $\boldsymbol{\sigma}$ by 1 and uses the resulting state as the top row and \mathbf{x}^{n-k+1} as the bottom row in the diagram like (VI) to produce a k -TAZRP state. Regarding \mathbf{x}^n as a 1-TAZRP state naturally, we have

$$\pi(\mathbf{x}^1 \otimes \dots \otimes \mathbf{x}^n) = \Phi_{n, \mathbf{x}^1} \circ \Phi_{n-1, \mathbf{x}^2} \circ \dots \circ \Phi_{2, \mathbf{x}^{n-1}}(\mathbf{x}^n).$$

This construction is a TAZRP analogue of the nested Bethe ansatz which diagonalizes the Hamiltonian of integrable $sl(n)$ spin chains inductively on n .

The algorithms explained in this subsection are the TAZRP counterpart of the multiple queueing process introduced for the TASEP [8]. Its reformulation by crystals and combinatorial R in [17] is quite parallel with the content here. They offer a unified perspective into the multispecies TAZRP and TASEP on the periodic chain \mathbb{Z}_L as the sister models corresponding to the symmetric and the antisymmetric tensor representations of the quantum affine algebra $U_q(\widehat{sl}_L)$ at $q = 0$.

4.5. Induced dynamics. We extend the map π (4.7) naturally to that on the space of states for n -line process and n -TAZRP $\pi : \bigoplus_{\mathbf{x} \in B(\mathbf{m})} \mathbb{C}|\mathbf{x}\rangle \rightarrow \bigoplus_{\boldsymbol{\sigma} \in S(\mathbf{m})} \mathbb{C}|\boldsymbol{\sigma}\rangle$ by linearity and $\pi(|\mathbf{x}\rangle) = |\pi(\mathbf{x})\rangle$. By the construction π is surjective. Recall that τ_i^k is defined around (2.4) and $T_{a,i}^k$ by (3.11) and (3.12).

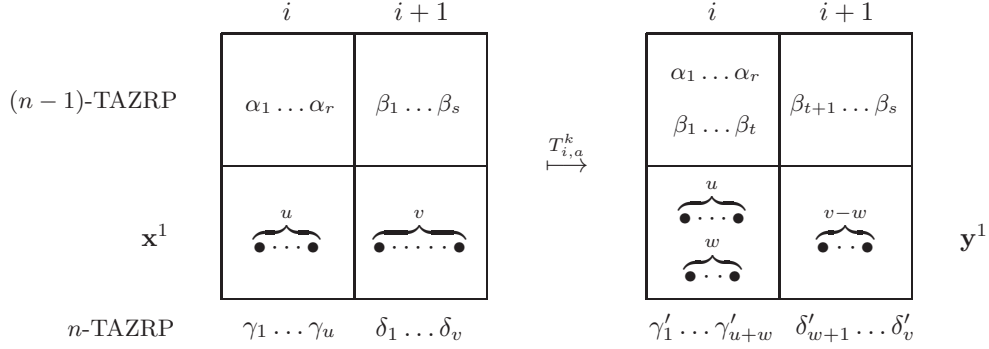
Proposition 4.6. *For $(i, a, k) \in \mathbb{Z}_L \times [1, n] \times \mathbb{Z}_{\geq 1}$, set $\tilde{\tau}_{i,a}^k = \tau_i^k$ for $a = 1$ and $\tilde{\tau}_{i,a}^k = 1$ for $a \in [2, n]$. Then the following diagram is commutative:*

$$\begin{array}{ccc} B(\mathbf{m}) & \xrightarrow{T_{i,a}^k} & B(\mathbf{m}) \\ \pi \downarrow & & \downarrow \pi \\ S(\mathbf{m}) & \xrightarrow{\tilde{\tau}_{i,a}^k} & S(\mathbf{m}) \end{array}$$

Proof. We invoke the induction on n . For $n = 1$ the claim is obvious. Assume the claim for $(n-1)$ -TAZRP. We utilize the description of π by the TAZRP embedding rule explained in the end of Section 4.4. Suppose $T_{i,a}^k : \mathbf{x}^1 \otimes \mathbf{x}^{\geq 2} \mapsto \mathbf{y}^1 \otimes \mathbf{y}^{\geq 2}$ with $\mathbf{x}^{\geq 2}, \mathbf{y}^{\geq 2} \in B_{\ell_2} \otimes \dots \otimes B_{\ell_n}$. Then $T_{i,a'}^{k'}(\mathbf{x}^{\geq 2}) = \mathbf{y}^{\geq 2}$ holds for $(n-1)$ -TAZRP states for some a' and k' . Set $\pi(\mathbf{x}^{\geq 2}) + 1 =$

⁴ This minor extra process can be avoided if the species a is replaced by $n+1-a$ everywhere.

$(\dots, \alpha_1 \dots \alpha_r, \beta_1 \dots \beta_s, \dots)$, where “+1” stands for the uniform increment of the species by 1, and $\alpha_1 \dots \alpha_r$ and $\beta_1 \dots \beta_s$ are the resulting $(n-1)$ -TAZRP local states (with species from $[2, n]$) at the i -th and the $(i+1)$ -th site, respectively. In particular $2 \leq \beta_1 \leq \dots \leq \beta_s \leq n$. Set $\mathbf{x}^1 = (\dots, u, v, \dots)$ similarly exhibiting the i -th and the $(i+1)$ -th components. By the induction assumption we know $\pi(\mathbf{y}^{\geq 2}) + 1 = (\dots, \alpha_1 \dots \alpha_r, \beta_1 \dots \beta_t, \beta_{t+1} \dots \beta_s, \dots)$ for some $t \in [0, s]$. From the definition of $T_{i,a}^k$ it follows that $\mathbf{y}^1 = (\dots, u+w, v-w, \dots)$ for some $w \in [0, v]$. Now the part of the diagram (V) in Section 4.4 corresponding to the i -th and the $(i+1)$ -th columns looks as follows.



We assume $2 \leq \delta_1 \leq \dots \leq \delta_v \leq n$. We are to draw H -lines from the particles in the top row to some dot in the bottom according to the TAZRP embedding rule in Section 4.4. To clarify the argument below, we assume that the H -line from a particle in the top row first goes down vertically, make 90° right turn in the box underneath and proceeds horizontally to the left periodically until it captures a yet unconnected dot in the bottom row. Thus in the bottom row of the above diagram, there are H -lines coming from the right of the $(i+1)$ -th box seeking the target dots and also the outgoing ones to the left of the i -th box. The new n -TAZRP particles γ'_j and δ'_j can be related to the previous ones γ_j and δ_j by inspecting the influence of the changes of the diagram on the H -lines. There are three cases to consider.

Case 1. $t \geq 1$ and $w = 0$. From (3.10) this happens only if $a = 2$ and $u \leq s - t$ with $k = t$. In the left diagram, the H -lines from $\beta_{s-u+1}, \dots, \beta_s$ are captured by the u dots in the bottom left box. The other H -lines from $\beta_1, \dots, \beta_{s-u}$ are outgoing to the left of it. This situation is the same as the right diagram, showing that the relocation of the particles β_1, \dots, β_t causes no change in the result of the TAZRP embedding rule. Thus we find $\gamma'_j = \gamma_j$ and $\delta'_j = \delta_j$ in agreement with $\tilde{\tau}_{i,2}^k = 1$.

Case 2. $t = 0$ and $w \geq 1$. This happens only if $a = 1$ and $u \geq s$ with $k = w$. In the both diagram, the s H -lines from β_1, \dots, β_s are all captured by the dots in the bottom left box. Thus the H -lines outgoing to the left of the i -th box is the same. It implies that the H -lines coming from the right of the $(i+1)$ -th box are also unchanged. Since the particles with larger species have priority to find the partner dots in the TAZRP embedding rule, we have $\delta'_j = \delta_j$ for $j \in [w+1, v]$ and $\{\gamma'_j\} = \{\gamma_j\} \cup \{\delta_1, \dots, \delta_w\}$. This agrees with (2.4) for $\tau_i^k = \tilde{\tau}_{i,a=1}^k$.

Case 3. $t \geq 1$ and $w \geq 1$. This happens only if $a = 1$ and $s - t = u$ with $k = w$. In the both diagram, the u H -lines from $\beta_{t+1}, \dots, \beta_s$ are absorbed into the dots in the bottom left box, and the other ones from β_1, \dots, β_t are outgoing to the left of the i -th box. Then the rest of the argument is the same as Case 2. \square

Example 4.7. Consider the maps in Example 3.5. According to the definition (3.11), we have $T_{1,1}^1(\mathbf{x}), \dots, T_{3,1}^1(\mathbf{x}) \in B(2, 1, 2, 1)$ for \mathbf{x} given in Example 3.2. Their image by π are given by

$$\begin{aligned} \pi(T_{1,1}^1(\mathbf{x})) &= |33, \emptyset, 1124\rangle, & \pi(T_{2,1}^1(\mathbf{x})) &= |3, 13, 124\rangle, & \pi(T_{2,1}^2(\mathbf{x})) &= |3, 113, 24\rangle, \\ \pi(T_{2,1}^3(\mathbf{x})) &= |3, 1123, 4\rangle, & \pi(T_{2,1}^4(\mathbf{x})) &= |3, 11234, \emptyset\rangle, & \pi(T_{2,2}^1(\mathbf{x})) &= |3, 3, 1124\rangle, \\ \pi(T_{3,1}^1(\mathbf{x})) &= |\emptyset, 3, 11234\rangle. \end{aligned}$$

By the result of Example 4.3 on the same \mathbf{x} , the claim of Proposition 4.6 is rephrased as

$$\begin{aligned}\tau_1^1|3, 3, 1124\rangle &= |33, \emptyset, 1124\rangle, & \tau_2^1|3, 3, 1124\rangle &= |3, 13, 124\rangle, & \tau_2^2|3, 3, 1124\rangle &= |3, 113, 24\rangle, \\ \tau_2^3|3, 3, 1124\rangle &= |3, 1123, 4\rangle, & \tau_2^4|3, 3, 1124\rangle &= |3, 11234, \emptyset\rangle, & 1|3, 3, 1124\rangle &= |3, 3, 1124\rangle, \\ \tau_3^1|3, 3, 1124\rangle &= |\emptyset, 3, 11234\rangle.\end{aligned}$$

These relations agree with the definition (2.4).

Proposition 4.6 tells that the dynamics of n -TAZRP is exactly the one that is induced from n -line process via the map π . Now we state the first main result of the article.

Theorem 4.8 (Steady state of n -TAZRP). *The steady state $|\bar{P}_L(\mathbf{m})\rangle$ of n -TAZRP in the sector $S(\mathbf{m})$ is the image of the n -line process steady state $|\Omega(\mathbf{m})\rangle$ in Corollary 3.7 by π . Namely,*

$$|\bar{P}_L(\mathbf{m})\rangle = \pi|\Omega(\mathbf{m})\rangle = \sum_{\mathbf{x} \in B(\mathbf{m})} |\pi(\mathbf{x})\rangle.$$

Proof. By Proposition 4.6, the Markov matrix of n -TAZRP (2.7) is expressed as $H_{\text{TAZRP}} = \sum_{i \in \mathbb{Z}_L} \sum_{a=1}^n \sum_{k \geq 1} (\bar{\tau}_{i,a}^k - 1)$. Moreover the intertwining relation

$$\pi H_{\text{LP}} = H_{\text{TAZRP}} \pi$$

holds, where H_{LP} is the Markov matrix of n -line process (3.13). Thus we have $H_{\text{TAZRP}}|\bar{P}_L(\mathbf{m})\rangle = 0$ from Corollary 3.7. This proves the claim thanks to the uniqueness of the steady state. \square

Theorem 4.8 is an analogue of the combinatorial construction of the n -TASEP steady state [8] whose quantum group theoretical origin was uncovered in [17].

Before closing the section we note a simple consequence of Theorem 4.8. Consider the most localized configuration of the n -TAZRP $(\emptyset, \dots, \emptyset, \text{all})$ and its cyclic permutations which have the same probability. Here *all* means the assembly of all the ℓ_1 particles in the sector $S(\mathbf{m})$. See (3.1) for ℓ_a . It is easy to see

$$\pi^{-1}(\emptyset, \dots, \emptyset, \text{all}) = (0, \dots, 0, \ell_1) \otimes B_{\ell_2} \otimes \dots \otimes B_{\ell_n}.$$

Therefore we get

$$\mathbb{P}(\emptyset, \dots, \emptyset, \text{all}) = \prod_{a=2}^n \binom{L-1+\ell_a}{\ell_a} \quad (4.11)$$

in agreement with Example 2.1. This is the *largest* probability in the sector. Similarly we find

$$\mathbb{P}(*, \overbrace{\emptyset, \dots, \emptyset}^d, \sigma_{d+1}, \dots, \sigma_L) = \binom{d+\ell_2}{\ell_2} \prod_{a=3}^n \binom{L-1+\ell_a}{\ell_a}$$

if $\sigma_{d+1} \neq \emptyset$ and $\sigma_{d+1}, \dots, \sigma_L$ contain particle of species 1 only with $*$ being the rest.

5. FORMULAE FOR STEADY STATE PROBABILITY

5.1. Crystalline corner transfer matrix. Recall that the steady state of n -TAZRP on \mathbb{Z}_L in the sector $S(\mathbf{m})$ has the form (2.8). Theorem 4.8 tells that the steady state probability therein is expressed as

$$\mathbb{P}(\sigma) = \#\{\mathbf{x} \in B(\mathbf{m}) \mid \pi(\mathbf{x}) = \sigma\}. \quad (5.1)$$

Example 5.1. Consider 3-TAZRP on \mathbb{Z}_3 in the sector $S(1, 2, 1)$. Example 2.1 tells $\mathbb{P}(1, 2, 23) = 5$, where $(1, 2, 23)$ is multiset representation. In fact there are exactly 5 elements in $B(1, 2, 1)$ which are mapped by π to $(1, 2, 23)$. In the notation (3.5) they are given by

$$\begin{pmatrix} 1 & 0 & 0 \\ 3 & 0 & 0 \\ 1 & 1 & 2 \end{pmatrix}, \quad \begin{pmatrix} 0 & 1 & 0 \\ 3 & 0 & 0 \\ 1 & 1 & 2 \end{pmatrix}, \quad \begin{pmatrix} 0 & 0 & 1 \\ 3 & 0 & 0 \\ 1 & 1 & 2 \end{pmatrix}, \quad \begin{pmatrix} 0 & 1 & 0 \\ 2 & 0 & 1 \\ 1 & 1 & 2 \end{pmatrix}, \quad \begin{pmatrix} 0 & 0 & 1 \\ 2 & 0 & 1 \\ 1 & 1 & 2 \end{pmatrix}.$$

From (4.5) we see $\varphi \circ \pi = \pi^1 \otimes \cdots \otimes \pi^n$. Thus the condition $\pi(\mathbf{x}) = \boldsymbol{\sigma}$ in (5.1) is equivalent to $\pi^1(\mathbf{x}) \otimes \cdots \otimes \pi^n(\mathbf{x}) = \varphi(\boldsymbol{\sigma}) = \varphi^1(\boldsymbol{\sigma}) \otimes \cdots \otimes \varphi^n(\boldsymbol{\sigma})$. Therefore (5.1) is rewritten as

$$\mathbb{P}(\boldsymbol{\sigma}) = \#\{\mathbf{x} \in B(\mathbf{m}) \mid \pi^a(\mathbf{x}) = \varphi^a(\boldsymbol{\sigma}), \forall a \in [1, n]\}. \quad (5.2)$$

To proceed we find it convenient to generalize the vertex diagram (4.3) for $R = R_{\ell, m}$ naturally to arbitrary edge states $\mathbf{a} = (a_1, \dots, a_L), \mathbf{i} = (i_1, \dots, i_L) \in B_\ell$ and $\mathbf{b} = (b_1, \dots, b_L), \mathbf{j} = (j_1, \dots, j_L) \in B_m$ as

$$\mathbf{i} \begin{array}{c} \uparrow \mathbf{b} \\ \text{---} \\ \text{---} \\ \downarrow \mathbf{j} \end{array} \mathbf{a} = R_{\mathbf{i}, \mathbf{j}}^{\mathbf{a}, \mathbf{b}} = \begin{cases} 1 & \text{if } R(\mathbf{i} \otimes \mathbf{j}) = \mathbf{b} \otimes \mathbf{a}, \\ 0 & \text{otherwise.} \end{cases} \quad (5.3)$$

By the definition $R_{\mathbf{i}, \mathbf{j}}^{\mathbf{a}, \mathbf{b}} = 0$ unless $\mathbf{a} + \mathbf{b} = \mathbf{i} + \mathbf{j}$. This property generalizing the ice rule in the six-vertex model [1] will be referred to as the *weight conservation*. The matrix element $R_{\mathbf{i}, \mathbf{j}}^{\mathbf{a}, \mathbf{b}}$ is nothing but the Boltzmann weight of the local vertex configuration at $q = 0$. Concatenations of the vertices in diagrams are naturally interpreted as configuration sums. With this convention we have

Theorem 5.2 (Corner transfer matrix formula). *The steady state probability $\mathbb{P}(\boldsymbol{\sigma})$ of n -TAZRP in the sector $S(\mathbf{m})$ is expressed as*

$$\mathbb{P}(\boldsymbol{\sigma}) = \sum_{\mathbf{x}^1 \otimes \cdots \otimes \mathbf{x}^n \in B(\mathbf{m})} \begin{array}{c} \varphi^n(\boldsymbol{\sigma}) \rightarrow \\ \vdots \\ \varphi^2(\boldsymbol{\sigma}) \rightarrow \\ \varphi^1(\boldsymbol{\sigma}) \rightarrow \\ \left. \begin{array}{c} \text{---} \\ \text{---} \\ \text{---} \end{array} \right\} \begin{array}{c} \mathbf{x}^1 \\ \mathbf{x}^2 \\ \dots \\ \mathbf{x}^n \end{array} \end{array}$$

The right hand side stands for the configuration sum under the boundary condition specified by $\varphi^1(\boldsymbol{\sigma}), \dots, \varphi^n(\boldsymbol{\sigma})$.

Proof. Follows from (5.2) and (4.10). \square

Example 5.3. Consider the 3-TAZRP on \mathbb{Z}_3 in the sector $S(1, 2, 1)$, which is the same as Example 5.1. We have $\varphi(1, 2, 23) = 112 \otimes 012 \otimes 001$ according to the rule illustrated in Example 4.2. By using them as the boundary condition, $\mathbb{P}(1, 2, 23) = 5$ is derived as the following sum corresponding to the 5 elements $\mathbf{x}^1 \otimes \mathbf{x}^2 \otimes \mathbf{x}^3 \in B(1, 2, 1)$ in Example 5.1.

$$\begin{array}{c} \begin{array}{c} \begin{array}{c} \text{---} \\ \text{---} \\ \text{---} \end{array} \begin{array}{c} \mathbf{u} \\ \mathbf{w} \end{array} \begin{array}{c} \rightarrow 001 \\ \rightarrow 111 \\ \rightarrow 400 \end{array} \\ 112 \quad 300 \quad 100 \end{array} + \begin{array}{c} \begin{array}{c} \text{---} \\ \text{---} \\ \text{---} \end{array} \begin{array}{c} \mathbf{u} \\ \mathbf{w} \end{array} \begin{array}{c} \rightarrow 001 \\ \rightarrow 111 \\ \rightarrow 310 \end{array} \\ 112 \quad 300 \quad 010 \end{array} + \begin{array}{c} \begin{array}{c} \text{---} \\ \text{---} \\ \text{---} \end{array} \begin{array}{c} \mathbf{u} \\ \mathbf{w} \end{array} \begin{array}{c} \rightarrow 001 \\ \rightarrow 111 \\ \rightarrow 301 \end{array} \\ 112 \quad 300 \quad 001 \end{array} + \begin{array}{c} \begin{array}{c} \text{---} \\ \text{---} \\ \text{---} \end{array} \begin{array}{c} \mathbf{v} \\ \mathbf{w} \end{array} \begin{array}{c} \rightarrow 001 \\ \rightarrow 111 \\ \rightarrow 211 \end{array} \\ 112 \quad 201 \quad 010 \end{array} + \begin{array}{c} \begin{array}{c} \text{---} \\ \text{---} \\ \text{---} \end{array} \begin{array}{c} \mathbf{v} \\ \mathbf{w} \end{array} \begin{array}{c} \rightarrow 001 \\ \rightarrow 111 \\ \rightarrow 202 \end{array} \\ 112 \quad 201 \quad 001 \end{array} \end{array}$$

Here we have set $\mathbf{u} = 400 \in B_4, \mathbf{v} = 301 \in B_4$ and $\mathbf{w} = 001 \in B_1$.

5.2. Factorization of combinatorial R . As a preparation for the next subsection, we present a matrix product formula for the combinatorial R . Let $F = \bigoplus_{m \geq 0} \mathbb{C}|m\rangle$ be a Fock space and $F^* = \bigoplus_{m \geq 0} \mathbb{C}\langle m|$ be its dual with the bilinear pairing such that $\langle m|m'\rangle = \delta_{m, m'}$ ⁵. Let further $\mathbf{a}^+, \mathbf{a}^-, \mathbf{k}$ be the linear operators acting on them as ($\langle -1| = |-1\rangle = 0$)

$$\begin{aligned} \mathbf{a}^+|m\rangle &= |m+1\rangle, & \mathbf{a}^-|m\rangle &= |m-1\rangle, & \mathbf{k}|m\rangle &= \delta_{m,0}|m\rangle, \\ \langle m|\mathbf{a}^+ &= \langle m-1|, & \langle m|\mathbf{a}^- &= \langle m+1|, & \langle m|\mathbf{k} &= \delta_{m,0}\langle m|. \end{aligned}$$

⁵Ket vectors here containing a single integer should not be confused with n -line states $|\mathbf{x}\rangle$ nor n -TAZRP states $|\boldsymbol{\sigma}\rangle$.

They satisfy the relations

$$\mathbf{k}^2 = \mathbf{k}, \quad \mathbf{k}\mathbf{a}^+ = 0, \quad \mathbf{a}^-\mathbf{k} = 0, \quad \mathbf{a}^-\mathbf{a}^+ = 1, \quad \mathbf{a}^+\mathbf{a}^- = 1 - \mathbf{k}, \quad (5.4)$$

which coincide with the q -oscillator algebra \mathcal{A}_q at $q = 0$ [17, (2.16)]. In this sense we refer to $\mathbf{a}^+, \mathbf{a}^-, \mathbf{k}$ as $q = 0$ -oscillators and (5.4) as $q = 0$ -oscillator algebra \mathcal{A}_0 . The equality $(\langle m|X|m'\rangle = \langle m|(X|m'\rangle))$ holds for any $X \in \mathcal{A}_0$. The \mathcal{A}_0 has a basis

$$1, \quad (\mathbf{a}^+)^r, \quad (\mathbf{a}^-)^r, \quad (\mathbf{a}^+)^s \mathbf{k} (\mathbf{a}^-)^t \quad (r \in \mathbb{Z}_{\geq 1}, s, t \in \mathbb{Z}_{\geq 0}). \quad (5.5)$$

Let $\mathcal{A}_0^{\text{fin}} \subset \mathcal{A}_0$ be the vector subspace spanned by (5.5) except 1. Then $\text{Tr}(X) := \sum_{m \geq 0} \langle m|X|m\rangle$ is finite for any $X \in \mathcal{A}_0^{\text{fin}}$.

Introduce the operator $\hat{R}_{i,j}^{a,b} \in \text{End}(F)$ together with its diagram representation as

$$\hat{R}_{i,j}^{a,b} = \begin{array}{c} b \\ \uparrow \\ i \text{---} \times \text{---} a \\ \downarrow \\ j \end{array} = \delta_{i+j}^{a+b} \theta(a \geq j) (\mathbf{a}^+)^j \mathbf{k}^{\theta(a > j)} (\mathbf{a}^-)^b \quad (a, b, i, j \in \mathbb{Z}_{\geq 0}), \quad (5.6)$$

where $\delta_i^a = \delta_{a,i}$. The blue arrow carries the Fock space on which the $q = 0$ -oscillators act. The other thin arrows carrying $\mathbb{Z}_{\geq 0}$ should not be confused with the thick arrows in (5.3) carrying the elements of crystals.

Lemma 5.4. *The matrix element $R_{ijk}^{abc} := \langle c|\hat{R}_{i,j}^{a,b}|k\rangle$ is expressed as*

$$R_{ijk}^{abc} = \begin{array}{c} b \\ \uparrow \\ i \text{---} \times \text{---} k \\ \downarrow \\ c \text{---} \times \text{---} a \\ \downarrow \\ j \end{array} = \delta_{j+(i-k)_+}^a \delta_{\min(i,k)}^b \delta_{j+(k-i)_+}^c,$$

where the symbol $(x)_+$ was defined in the beginning of Section 3.2.

Proof. Substituting $\theta(a \geq j) = \delta_j^a + \theta(a > j)$ into (5.6) we find

$$\begin{aligned} R_{ijk}^{abc} &= \delta_{i+j}^{a+b} \delta_j^a \langle c|(\mathbf{a}^+)^j (\mathbf{a}^-)^b|k\rangle + \delta_{i+j}^{a+b} \theta(a > j) \langle c|(\mathbf{a}^+)^j \mathbf{k} (\mathbf{a}^-)^b|k\rangle \\ &= \delta_{i+j}^{a+b} \delta_j^a \delta_{k-b+j}^c \theta(k \geq b) + \delta_{i+j}^{a+b} \theta(a > j) \delta_k^b \delta_j^c \\ &= \delta_j^a \delta_i^b \delta_{k-i+j}^c \theta(k \geq i) + \delta_{i+j-k}^a \delta_k^b \delta_j^c \theta(k < i). \end{aligned} \quad (5.7)$$

□

Note that

$$R_{ijk}^{abc} = 0 \quad \text{unless} \quad (a+b, b+c) = (i+j, j+k). \quad (5.8)$$

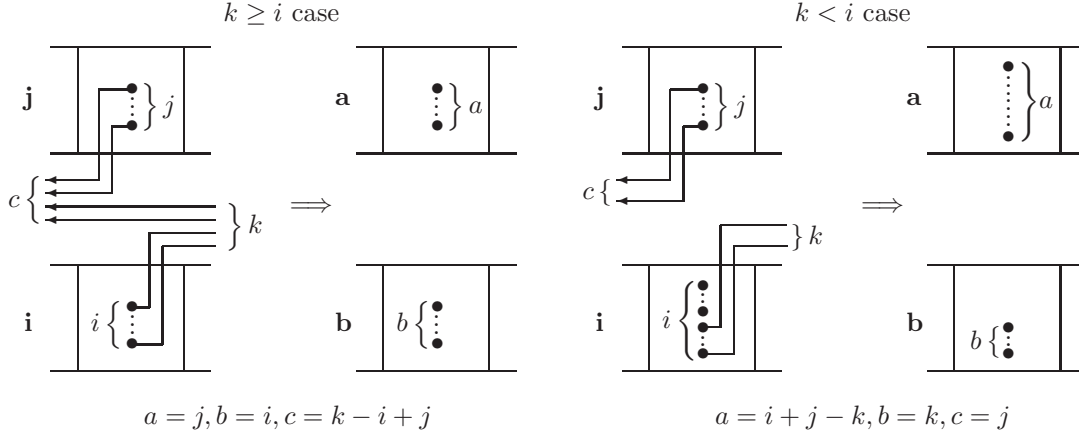
Proposition 5.5 (Matrix product form of combinatorial R). *Let $\mathbf{a} = (a_1, \dots, a_L), \mathbf{i} = (i_1, \dots, i_L) \in B_\ell$ and $\mathbf{b} = (b_1, \dots, b_L), \mathbf{j} = (j_1, \dots, j_L) \in B_m$. The matrix element (5.3) of the combinatorial $R_{\ell,m}$ with $\ell > m$ is expressed as*

$$R_{\mathbf{i},\mathbf{j}}^{\mathbf{a},\mathbf{b}} = \begin{array}{c} \mathbf{b} \\ \uparrow \\ \mathbf{i} \text{---} \times \text{---} \mathbf{a} \\ \downarrow \\ \mathbf{j} \end{array} = \text{Tr} \left(\begin{array}{c} b_L \\ \uparrow \\ i_L \text{---} \times \text{---} a_L \\ \downarrow \\ j_L \end{array} \dots \begin{array}{c} b_2 \\ \uparrow \\ i_2 \text{---} \times \text{---} a_2 \\ \downarrow \\ j_2 \end{array} \dots \begin{array}{c} b_1 \\ \uparrow \\ i_1 \text{---} \times \text{---} a_1 \\ \downarrow \\ j_1 \end{array} \right) = \text{Tr}(\hat{R}_{i_1, j_1}^{a_1, b_1} \dots \hat{R}_{i_L, j_L}^{a_L, b_L}).$$

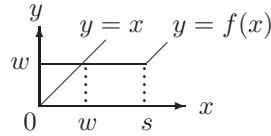
Proof. We are to show

$$R_{\mathbf{i}, \mathbf{j}}^{\mathbf{a}, \mathbf{b}} = \sum_{c_1, \dots, c_L} R_{i_1 j_1 c_1}^{a_1 b_1 c_L} R_{i_2 j_2 c_2}^{a_2 b_2 c_1} \dots R_{i_L j_L c_L}^{a_L b_L c_{L-1}}.$$

The left hand side is 1 or 0 depending on whether $R(\mathbf{i} \otimes \mathbf{j}) = \mathbf{b} \otimes \mathbf{a}$ or not according to the NY-rule in Section 4.1. The right hand side is the sum over $c_1, \dots, c_L \in \mathbb{Z}_{\geq 0}$ which effectively reduces to a *single* sum due to (5.8) and $\sum_r (a_r, b_r) = \sum_r (i_r, j_r) = (l, m)$. Consider the dot diagrams in the NY-rule for $\mathbf{i}, \mathbf{j}, \mathbf{a}, \mathbf{b}$ and their r -th boxes from the left which contain i_r, j_r, a_r, b_r dots, respectively. We are going to identify c_r (resp. c_{r-1}) with the numbers of H -lines coming from the right (resp. outgoing to the left) of these boxes. The identification is certainly consistent locally since (5.7) agrees with the NY-rule depicted below under the abbreviation $(a, b, c, i, j, k) = (a_r, b_r, c_{r-1}, i_r, j_r, c_r)$.



It remains to show that for any given $\mathbf{i} \otimes \mathbf{j} \in B_\ell \otimes B_m$ with $\ell > m$, there is a unique solution (c_1, \dots, c_L) to the simultaneous equations $c_{r-1} = j_r + (c_r - i_r)_+$ with $r \in [1, L]$ and $c_0 = c_L$. They are postulated from the rightmost factor $\delta_{j_+(k-i)_+}^c$ in Lemma 5.4 and the cyclicity of the trace. From the relations $c_{r-1} = j_r + (c_r - i_r)_+$ with $r \in [1, L]$, we have a piecewise linear expression $c_0 = f(c_L)$ in terms of c_L including \mathbf{i} and \mathbf{j} as parameters. We are to verify that $x = f(x)$ has a unique solution. In fact it is given by $x = w := f(0)$. To see this note that $f(x+1) = f(x)$ or $f(x) + 1$ because of $(x+1)_+ = (x)_+$ or $(x)_+ + 1$. Let s be the smallest nonnegative integer such that $f(s) = w$ and $f(s+1) = w+1$. This can happen only if $c_{r-1} = c_r + j_r - i_r$ holds for all $r \in [1, L]$ upon the choice $c_L = s$. Then $f(s) = s + \sum_{r=1}^L (j_r - i_r) = s + m - \ell$. Thus $f(s) = w$ forces $w < s$ by the assumption $\ell > m$. Now the unique existence of the solution to $x = f(x)$ is obvious from the following graph.



□

From the proof it also follows that $R_{i_1, j_1}^{a_1, b_1} \dots R_{i_L, j_L}^{a_L, b_L} \in \mathcal{A}_0^{\text{fin}}$ and its trace is convergent. In fact this fact can directly be derived from (5.6) since there is at least one r such that $\theta(a_r > j_r) = 1$ due to $\mathbf{a} \in B_\ell, \mathbf{j} \in B_m$ and $\ell - m > 0$.

Proposition 5.5 is a special case $\forall \epsilon_r = 0$ of [16, Th.6] and is also a corollary of [20, Th.4.1] at $q = 0$. The operator $R \in \text{End}(F^{\otimes 3})$ defined by $R(|i\rangle \otimes |j\rangle \otimes |k\rangle) = \sum_{a,b,c} R_{ijk}^{abc} |a\rangle \otimes |b\rangle \otimes |c\rangle$ using R_{ijk}^{abc} in Lemma 5.4 is known to satisfy the tetrahedron equation $R_{1,2,4} R_{1,3,5} R_{2,3,6} R_{4,5,6} = R_{4,5,6} R_{2,3,6} R_{1,3,5} R_{1,2,4}$ [25]. Furthermore this R is the $q = 0$ limit of the 3D R operator including generic q , which has a long history going back to [13]. See for example [2, 20, 16] and references

therein. We will present a new application of the 3D R operator and the tetrahedron equation to n -TAZRP in [19].

Example 5.6. We calculate two elements of the combinatorial $R: B_4 \otimes B_3 \rightarrow B_3 \otimes B_4$ according to Proposition 5.5.

$$\begin{aligned} R_{0121,1101}^{1201,0021} &= \text{Tr}(R_{0,1}^{1,0} R_{1,1}^{2,0} R_{2,0}^{0,2} R_{1,1}^{1,1}) = \text{Tr}(\mathbf{a}^+ \mathbf{a}^+ \mathbf{k} (\mathbf{a}^-)^2 \mathbf{a}^+ \mathbf{a}^-) = \langle 0 | (\mathbf{a}^-)^2 \mathbf{a}^+ \mathbf{a}^- \mathbf{a}^+ \mathbf{a}^+ | 0 \rangle = 1, \\ R_{0121,1101}^{1111,0111} &= \text{Tr}(R_{0,1}^{1,0} R_{1,1}^{1,1} R_{2,0}^{1,1} R_{1,1}^{1,1}) = \text{Tr}(\mathbf{a}^+ \mathbf{a}^+ \mathbf{a}^- \mathbf{k} \mathbf{a}^- \mathbf{a}^+ \mathbf{a}^-) = \langle 0 | \mathbf{a}^- \mathbf{a}^+ \mathbf{a}^- \mathbf{a}^+ \mathbf{a}^+ \mathbf{a}^- | 0 \rangle = 0. \end{aligned}$$

The both elements satisfy the weight conservation, but the one matching the combinatorial R is the former. It coincides with the bottom left vertex in the left hand side of (4.4).

5.3. Matrix product formula for steady state probability. One may regard $\hat{R}_{i,j}^{a,b}$ (5.6) as the \mathcal{A}_0 -valued Boltzmann weight of a 2D vertex model. Depict it omitting the blue arrow as

$$\hat{R}_{i,j}^{a,b} = i \begin{array}{c} b \\ \uparrow \\ \text{---} \\ \downarrow \\ j \\ a \end{array} = \delta_{i+j}^{a+b} \theta(a \geq j) (\mathbf{a}^+)^j \mathbf{k}^{\theta(a > j)} (\mathbf{a}^-)^b. \quad (5.9)$$

This vertex $\hat{R}_{i,j}^{a,b}$ made of thin arrows carrying $a, b, i, j \in \mathbb{Z}_{\geq 0}$ should be distinguished from $R_{\mathbf{i},\mathbf{j}}^{\mathbf{a},\mathbf{b}}$ in (5.3) which consists of thick arrows carrying $\mathbf{a}, \mathbf{i} \in B_\ell$ and $\mathbf{b}, \mathbf{j} \in B_m$. The factor δ_{i+j}^{a+b} in (5.9) represents an ice type conservation rule. Although it is a vertex model whose local states range over the infinite set $\mathbb{Z}_{\geq 0}$, the quantities relevant to n -TAZRP become finite as we will see below.

Recall that a local state σ_i of n -TAZRP at site $i \in \mathbb{Z}_L$ has the form $\sigma_i = (\sigma_i^1, \dots, \sigma_i^n)$ in multiplicity representation as in (2.1). With such an array $\sigma = (\sigma^1, \dots, \sigma^n) \in (\mathbb{Z}_{\geq 0})^n$ we associate the operator $X_\sigma \in \text{End}(F^{\otimes n(n-1)/2})$ defined by

$$X_\sigma = X_{\sigma^1, \dots, \sigma^n} = \sum \begin{array}{c} \sigma^n \\ \rightarrow \\ \sigma^{n-1} + \sigma^n \\ \rightarrow \\ \vdots \\ \rightarrow \\ \sigma^1 + \dots + \sigma^n \\ \rightarrow \end{array} \quad (5.10)$$

This is a configuration sum of the \mathcal{A}_0 -valued vertex model defined by (5.9). Each edge ranges over $\mathbb{Z}_{\geq 0}$ with the fixed boundary condition on the diagonal and the free boundary condition on the bottom row and the rightmost column. The summand represents a *tensor product* of the $q = 0$ -oscillator operators (5.9) attached to the vertices. The diagram has the same structure as that in Proposition 5.2. Note however that the thick arrows there carry elements of crystals whereas the thin arrows here do just nonnegative integers. In short the X_σ is a corner transfer matrix of the \mathcal{A}_0 -valued vertex model⁶.

Example 5.7. For $n = 2$ the operator X_σ with $\sigma = (\sigma^1, \sigma^2)$ is given by

$$X_{\sigma^1, \sigma^2} = \sum_j \sigma^1 + \sigma^2 \begin{array}{c} \sigma^2 \\ \rightarrow \\ \text{---} \\ \downarrow \\ j \\ \sigma^1 \end{array} j + \sigma^1 = \sum_{j \geq 0} (\mathbf{a}^+)^j \mathbf{k}^{\sigma^1} (\mathbf{a}^-)^{\sigma^2}.$$

⁶ Actually the sum of elements of the corner transfer matrix in the original sense [1] since we employ the free boundary condition on the bottom row and the rightmost column.

For $n = 3$ the operator X_σ with $\sigma = (\sigma^1, \sigma^2, \sigma^3)$ is given by

$$\begin{aligned}
X_{\sigma^1, \sigma^2, \sigma^3} &= \sum_{i, j, k} \sigma^1 + \sigma^2 + \sigma^3 \begin{array}{c} \xrightarrow{\sigma^3} \\ \begin{array}{|c|} \hline \xrightarrow{\sigma^2 + \sigma^3} \\ \hline \end{array} \\ \begin{array}{|c|} \hline \xrightarrow{k} \\ \hline \end{array} \\ \begin{array}{|c|} \hline \xrightarrow{i} \\ \hline \end{array} \\ \begin{array}{|c|} \hline \xrightarrow{j} \\ \hline \end{array} \\ \hline \end{array} \\
&= \sum_{i, j, k} (\mathbf{a}^+)^j \mathbf{k}^{\sigma^1 + i - k} (\mathbf{a}^-)^k \otimes (\mathbf{a}^+)^k \mathbf{k}^{\sigma^2} (\mathbf{a}^-)^{\sigma^3} \otimes (\mathbf{a}^+)^i \mathbf{k}^{\sigma^1} (\mathbf{a}^-)^{\sigma^2 + \sigma^3},
\end{aligned}$$

where the sum extends over $i, j \in \mathbb{Z}_{\geq 0}$ and $k \in [0, \sigma^1 + i]$. Components of the tensor product corresponding to the three vertices have been ordered as (bottom right) \otimes (top right) \otimes (bottom left).

As seen in these examples, X_σ is an infinite sum in general. However the following formula, which is our second main result in this article, is divergence-free.

Theorem 5.8 (Matrix product formula for steady state probability of n -TAZRP). *The steady state probability of the configuration $(\sigma_1, \dots, \sigma_L)$ of n -TAZRP on the periodic chain \mathbb{Z}_L is expressed as*

$$\mathbb{P}(\sigma_1, \dots, \sigma_L) = \text{Tr}(X_{\sigma_1} \cdots X_{\sigma_L}),$$

where the trace is taken over $F^{\otimes n(n-1)/2}$.

Proof. Substitute Proposition 5.5 into Theorem 5.2 and use the definitions (4.5) and (5.10). \square

Convergence of the trace is guaranteed by the equivalence to Theorem 5.2 which is manifestly finite.

Example 5.9. Consider 2-TAZRP on \mathbb{Z}_4 in the sector $S(1, 1)$. Translating the configurations e.g. $(\emptyset, \emptyset, 1, 2)$ in multiset representation into multiplicity representation $(00, 00, 10, 01)$, we have

$$\begin{aligned}
\mathbb{P}(\emptyset, \emptyset, \emptyset, 12) &= \mathbb{P}(00, 00, 00, 11) = \text{Tr}(X_{00} X_{00} X_{00} X_{11}) = \sum \text{Tr}((\mathbf{a}^+)^{j_1 + j_2 + j_3 + j_4} \mathbf{k} \mathbf{a}^-) = 4, \\
\mathbb{P}(\emptyset, \emptyset, 1, 2) &= \mathbb{P}(00, 00, 10, 01) = \text{Tr}(X_{00} X_{00} X_{10} X_{01}) = \sum \text{Tr}((\mathbf{a}^+)^{j_1 + j_2 + j_3} \mathbf{k} (\mathbf{a}^+)^{j_4} \mathbf{a}^-) = 3, \\
\mathbb{P}(\emptyset, 1, \emptyset, 2) &= \mathbb{P}(00, 10, 00, 01) = \text{Tr}(X_{00} X_{10} X_{00} X_{01}) = \sum \text{Tr}((\mathbf{a}^+)^{j_1 + j_2} \mathbf{k} (\mathbf{a}^+)^{j_3 + j_4} \mathbf{a}^-) = 2, \\
\mathbb{P}(\emptyset, \emptyset, 2, 1) &= \mathbb{P}(00, 00, 01, 10) = \text{Tr}(X_{00} X_{00} X_{01} X_{10}) = \sum \text{Tr}((\mathbf{a}^+)^{j_1 + j_2 + j_3} \mathbf{a}^- (\mathbf{a}^+)^{j_4} \mathbf{k}) = 1,
\end{aligned}$$

where the operators X_{σ^1, σ^2} are taken from Example 5.7. The sum is over $j_1, \dots, j_4 \in \mathbb{Z}_{\geq 0}$. They agree with $|\xi_4(1, 1)\rangle$ in Example 2.1.

Example 5.10. Similarly for 3-TAZRP on \mathbb{Z}_3 in the sector $S(1, 2, 1)$ we have

$$\begin{aligned}
\mathbb{P}(1, 2, 23) &= \mathbb{P}(100, 010, 011) = \text{Tr}(X_{100} X_{010} X_{011}) = \sum \text{Tr}(Y_1) \text{Tr}(Y_2) \text{Tr}(Y_3), \\
Y_1 &= (\mathbf{a}^+)^{j_1} \mathbf{k}^{1+i_1-k_1} (\mathbf{a}^-)^{k_1} (\mathbf{a}^+)^{j_2} \mathbf{k}^{i_2-k_2} (\mathbf{a}^-)^{k_2} (\mathbf{a}^+)^{j_3} \mathbf{k}^{i_3-k_3} (\mathbf{a}^-)^{k_3}, \\
Y_2 &= (\mathbf{a}^+)^{k_1} (\mathbf{a}^+)^{k_2} \mathbf{k} (\mathbf{a}^+)^{k_3} \mathbf{k} \mathbf{a}^-, \\
Y_3 &= (\mathbf{a}^+)^{i_1} \mathbf{k} (\mathbf{a}^+)^{i_2} \mathbf{a}^- (\mathbf{a}^+)^{i_3} (\mathbf{a}^-)^2,
\end{aligned}$$

where the operators $X_{\sigma^1, \sigma^2, \sigma^3}$ are again taken from Example 5.7. The sum is over i_r, j_r, k_r ($r = 1, 2, 3$) $\in \mathbb{Z}_{\geq 0}$ under the condition that all the powers of \mathbf{k} in Y_1 are nonnegative. There are five such choices yielding the nonvanishing summands as

$$\begin{pmatrix} i_1 & j_1 & k_1 \\ i_2 & j_2 & k_2 \\ i_3 & j_3 & k_3 \end{pmatrix} = \begin{pmatrix} 3 & 1 & 1 \\ 0 & 0 & 0 \\ 0 & 0 & 0 \end{pmatrix}, \begin{pmatrix} 3 & 0 & 1 \\ 0 & 1 & 0 \\ 0 & 0 & 0 \end{pmatrix}, \begin{pmatrix} 3 & 0 & 1 \\ 0 & 0 & 0 \\ 0 & 1 & 0 \end{pmatrix}, \begin{pmatrix} 2 & 0 & 1 \\ 0 & 1 & 0 \\ 1 & 0 & 0 \end{pmatrix}, \begin{pmatrix} 2 & 0 & 1 \\ 0 & 0 & 0 \\ 1 & 1 & 0 \end{pmatrix}.$$

Each of them contributes by 1, reproducing the result $\mathbb{P}(1, 2, 23) = 5$ in agreement with $|\xi_3(1, 2, 1)\rangle$ in Example 2.1 and Example 5.3.

ACKNOWLEDGMENTS

This work is supported by Grants-in-Aid for Scientific Research No. 15K04892, No. 15K13429 and No. 23340007 from JSPS.

REFERENCES

- [1] R. J. Baxter, *Exactly solved models in statistical mechanics*, Dover (2007).
- [2] V. V. Bazhanov and S. M. Sergeev, Zamolodchikov’s tetrahedron equation and hidden structure of quantum groups, *J. Phys. A: Math. Gen.* **39** (2006) 3295–3310.
- [3] A. Borodin, I. Corwin and T. Sasamoto, From duality to determinants for q -TASEP and ASEP. *Ann. Probab.* **42** (2014) 2314–2382.
- [4] E. Date, M. Jimbo, A. Kuniba, T. Miwa and M. Okado, Exactly solvable SOS models, Local height probabilities and theta function identities, *Nucl. Phys. B* **290** [FS20] (1987) 231–273.
- [5] V. G. Drinfeld, Hopf algebras and the quantum Yang-Baxter equation, *Soviet Math. Doklady* **32** (1985) 254–258.
- [6] V. G. Drinfeld, On some unsolved problems in quantum group theory. In “Quantum groups”, *Lect. Notes in Math.* **1510** (1992) p1–8.
- [7] M. R. Evans and T. Hanney, Nonequilibrium statistical mechanics of the zero-range process and related models, *J. Phys. A: Math. Gen.* **38** (2005) R195–R240.
- [8] P. A. Ferrari and J. B. Martin, Stationary distributions of multi-type totally asymmetric exclusion processes, *Ann. Probab.* **35** (2007) 807–832.
- [9] G. Hatayama, A. Kuniba, M. Okado, T. Takagi and Z. Tsuboi, Paths, crystals and Fermionic formulae, *Prog. in Math. Phys.* **23** Birkhäuser (2002) p205–272.
- [10] J. Hong and S-J. Kang, *Introduction to quantum groups and crystal bases*, Graduate Studies in Math. **42**, AMS (2002).
- [11] R. Inoue, A. Kuniba and T. Takagi, Integrable structure of box-ball systems: crystal, Bethe ansatz, ultradiscretization and tropical geometry, *J. Phys. A: Math. Theor.* **45** (2012) 073001 (64pp).
- [12] M. Jimbo, A q -difference analogue of $U(\mathfrak{g})$ and the Yang-Baxter equation, *Lett. Math. Phys.* **10** (1985) 63–69.
- [13] M. M. Kapranov and V. A. Voevodsky, 2-Categories and Zamolodchikov tetrahedron equations in *Proc. Symposia in Pure Mathematics* **56** (1994) 177–259.
- [14] M. Kashiwara, On crystal bases of q -analogue of universal enveloping algebras, *Duke Math. J.* **63** (1991) 465–516.
- [15] S-J. Kang, M. Kashiwara, K. C. Misra, T. Miwa, T. Nakashima and A. Nakayashiki, Affine crystals and vertex models, *Int. J. Mod. Phys. A* **7** (suppl. 1A) (1992) 449–484.
- [16] A. Kuniba, Combinatorial Yang-Baxter maps arising from tetrahedron equation, preprint arXiv:1509.02245, to appear in *Theor. Math. Phys.* **189**(1): (2016) 1472–1485.
- [17] A. Kuniba, S. Maruyama and M. Okado, Multispecies TASEP and combinatorial R , *J. Phys. A: Math. Theor.* **48** (2015) 34FT02 (19pp).
- [18] A. Kuniba, S. Maruyama and M. Okado, Multispecies TASEP and the tetrahedron equation, *J. Phys. A: Math. Theor.* **49** (2016) 114001 (22pp).
- [19] A. Kuniba, S. Maruyama and M. Okado, Multispecies totally asymmetric zero range process: II. Hat relation and tetrahedron equation, *J. Integrable Syst.* **1**(1): xyw008.
- [20] A. Kuniba, M. Okado and S. Sergeev, Tetrahedron equation and generalized quantum groups, *J. Phys. A: Math. Theor.* **48** (2015) 304001 (38pp).
- [21] A. Nakayashiki and Y. Yamada, Kostka polynomials and energy functions in solvable lattice models, *Selecta Mathematica, New Ser.* **3** (1997) 547–599.
- [22] A. M. Povolotsky, On the integrability of zero-range chipping models with factorized steady states, *J. Phys. A: Math. Theor.* **46** (2013) 465205 (25pp).
- [23] A. Veselov, Yang-Baxter maps: Dynamical point of view, *Math. Soc. Japan Memoirs* **17** (2007) 145–167.
- [24] Y. Yamada, Birational representation of Weyl group, combinatorial R -matrix and discrete Toda equation, in *Physics and Combinatorics*, Proceedings of the Nagoya 2000 International Workshop, A. N. Kirillov and N. Liskova, ed. World Scientific (2001), p305–319.
- [25] A. B. Zamolodchikov, Tetrahedra equations and integrable systems in three-dimensional space, *Soviet Phys. JETP* **79** 641–664 (1980).

E-mail address: atsuo@gokutan.c.u-tokyo.ac.jp

INSTITUTE OF PHYSICS, UNIVERSITY OF TOKYO, KOMABA, TOKYO 153-8902, JAPAN

E-mail address: maruyama@gokutan.c.u-tokyo.ac.jp

INSTITUTE OF PHYSICS, UNIVERSITY OF TOKYO, KOMABA, TOKYO 153-8902, JAPAN

E-mail address: `okado@sci.osaka-cu.ac.jp`

DEPARTMENT OF MATHEMATICS, OSAKA CITY UNIVERSITY, 3-3-138, SUGIMOTO, SUMIYOSHI-KU, OSAKA, 558-8585, JAPAN